frontiers in Plant Science

ORIGINAL RESEARCH
published: 15 September 2020
doi: 10.3389/fpls.2020.571157

Photosynthesis Performance and Antioxidative Enzymes Response of *Melia azedarach* and *Ligustrum lucidum* Plants Under Pb–Zn Mine Tailing Conditions

XinHao Huang[1], *Fan Zhu*[1,2*], *ZhiXiang He*[1], *XiaoYong Chen*[2,3], *GuangJun Wang*[1,2], *MengShan Liu*[2] *and HongYang Xu*[2]

[1] College of Life Science and Technology, Central South University of Forestry and Technology, Changsha, China, [2] National Engineering Laboratory for Applied Forest Ecological Technology in Southern China, Central South University of Forestry and Technology, Changsha, China, [3] College of Arts and Sciences, Governors State University, University Park, IL, United States

OPEN ACCESS

Edited by:
Basharat Ali,
University of Agriculture, Faisalabad, Pakistan

Reviewed by:
Mujahid Farid,
University of Gujrat, Pakistan
Theodore Mulembo Mwamba,
Zhejiang University, China

***Correspondence:**
Fan Zhu
csuftzf@163.com

Specialty section:
This article was submitted to Plant Nutrition, a section of the journal Frontiers in Plant Science

Received: *12 June 2020*
Accepted: *27 August 2020*
Published: *15 September 2020*

Citation:
Huang X, Zhu F, He Z, Chen X, Wang G, Liu M and Xu H (2020) Photosynthesis Performance and Antioxidative Enzymes' Response of Melia azedarach and Ligustrum lucidum Plants Under Pb–Zn Mine Tailing Conditions. Front. Plant Sci. 11:571157. doi: 10.3389/fpls.2020.571157

Lead–zinc (Pb–Zn) mine tailings pose a great risk to the natural environment and human health because of their high toxicity. In this study, the responses of photosynthesis, chlorophyll fluorescence, and antioxidative enzyme of *Melia azedarach* and *Ligustrum lucidum* in the soil contaminated by Pb–Zn mine tailings were investigated. Results showed that Pb–Zn mine tailings significantly reduced net photosynthetic rates and leaf photosynthetic pigment content of both trees, and the reduction of net photosynthetic rates was mainly caused by their biochemical limitation (BL). The chlorophyll fluorescence parameters from Pb–Zn tailing stressed leaves indicated that Pb–Zn tailings affected PSII activity which was evident from the change values of energy fluxes per reaction center (RC): probability that an electron moves further than Q_A^- (ET_O/TR_O), maximum quantum yield for primary photochemistry (TR_O/ABS), the density of PSII RC per excited cross-section (RC/CS_O), the absorption of antenna chlorophylls per PSII RC (ABS/RC), and the turnover number of Q_A reduction events (N). Pb–Zn mine tailings also affected the oxidation and reduction of PSI, which resulted in a great increase of reactive oxygen species (ROS) contents and then stimulated the rate of lipid peroxidation. Both trees exhibited certain antioxidative defense mechanisms as elevated superoxide dismutase (SOD), peroxidase (POD), and catalase (CAT) activities, then declined under high level of Pb–Zn tailing treatment. Comparatively, *L. lucidum* showed less extent effect on photosynthesis and higher antioxidative enzyme activities than *M. azedarach*; thus *L. lucidum* was more tolerant than *M. azedarach* at least under the described Pb–Zn tailing treatment. These results indicate that the effect of Pb–Zn mine tailings on photosynthesis performance mainly related to imbalance of the PSII activity and PSI redox state in both trees. We propose that *M. azedarach* and *L. lucidum* could relieve the oxidative stress for phytoremediation under the appropriate Pb–Zn mine tailing content.

Keywords: antioxidative enzymes, *Ligustrum lucidum*, *Melia azedarach*, Pb–Zn tailings, photosynthesis

INTRODUCTION

Plants require certain heavy metals (HMs) as essential elements for their growth, development, and yield production, but excess amount of these metals can become phytotoxic and cause adverse effects on plant biomass production, crop yield, and food safety (Pierattini et al., 2017). The major sources of HMs originated from anthropogenic activities; mining activities seem to be the largest contributor of HM pollutions in many places, and it is a particular case in China (Ha et al., 2011; Han et al., 2013; Zhuang et al., 2014; Chen et al., 2015). It was recently reported that the mining activities have resulted in about 40,000 ha mining wastelands in this country, and the wastelands have been continuously expanded at a rate of 3,300 ha per year (Li, 2006; Luo et al., 2015; Yu et al., 2019). Mining activities generated a large amount of mine tailings in the mining sites where high concentrations of Pb, Zn, and other HMs were detected in local environments, which caused a wide range of environmental problems (Han et al., 2013). Therefore, it is urgent and necessary to reestablish vegetation in mining wasteland for ecological restoration (Yu et al., 2019).

Various methods have been identified and employed to the restoration of HM-polluted soils (Teng et al., 2015). Phytoremediation technology has been widely considered as an efficient, inexpensive, and environmental-friendly approach to clean up the contaminated environments by HMs (Han et al., 2016). Trees have the great potential use in remediation of HM-polluted soil in view of large biomass and massive root systems (Pulford and Watson, 2003). However, Tang et al. (2019) demonstrated that the Pb–Zn mine tailing significantly reduced plant growth and chlorophyll contents in three woody plants (*Castanopsis fissa*, *Daphniphyllum calycinum* and *Pinus massoniana*). The limitation in tree growth might thus be associated with photosynthesis which was sensitive to HM stress (Çiçek et al., 2017; Zhong et al., 2018; Huang et al., 2019; Liang et al., 2019). Evidence showed that the reduction of leaf photosynthesis under HM toxicity might be attributed to the limitation of stomatal opening (Gs) and CO_2 diffusion in mesophyll (Gm), the suppression of photochemistry and biochemistry, or synthetic combinations of these factors (Kosobrukhov et al., 2004; Kola and Wilkinson, 2005; Krantev et al., 2008; Deng et al., 2014). Sagardoy et al. (2010) reported the main limitation to photosynthesis rate in sugar beet was likely due to the reduction of Gs under Zn stress. Lin and Jin (2018) found similar results in an experiment with three vegetables (*B. chinensis*, *C. coronarium*, and *B. alboglabra*) under Cu stress. However, Velikova et al. (2011) studied the impact of Ni on the photosynthesis of *Populus nigra* and found the limitation to photosynthesis rates of this species resulted from the restriction in Gm, not in Gs. Gm influenced photosynthetic capacity and determined the available CO_2 concentration for photosynthesis in the chloroplasts (Centritto et al., 2009). Some studies showed that the electron transfer was inhibited by Pb pollutant at the photosystem I (PSI) donor side because Pb affected activity of PSI (Belatik et al., 2013; Bernardini et al., 2016), but some studies suggested the activity of PSI in *Microcystis aeruginosa* and *Chlorella pyrenoidosa* had no inhibition with Cd treatment (Zhou et al., 2006; Wang et al., 2013). And some studies indicated that Cd affected the whole electron transport in photosystem II (PSII): on the donor side, it inhibited the OEC, while on the acceptor side, it inhibited electron transport between Q_A^- and Q_B^-. (Mallick and Mohn, 2003; Sigfridsson et al., 2004; Chu et al., 2018). Additionally, a number of studies also reported that HMs exhibited less effect of photosynthetic rate, electron transport, conversion of light energy, and photochemical efficiency in tolerant plant species than those in sensitive ones (Guo et al., 2018; Sorrentino et al., 2018; Huang et al., 2019).

Reactive oxygen species (ROS) can highly increase in the chloroplasts when photosynthetic electron transport chain was blocked by HM toxicity (Zhang et al., 2018). ROS like superoxide (O_2^-) and hydrogen peroxide (H_2O_2) could lead to lipid peroxidation, protein oxidation, membrane and nucleic acid damage, and inactivation of enzymes (Bi et al., 2016; Bezerril et al., 2017; Lu et al., 2017). To prevent an oxidative damage, plants activated enzymatic ROS scavenging mechanisms, such as superoxide dismutase (SOD), peroxidase (POD) and catalase (CAT), ascorbic acid and glutathione, to keep ROS at a basal non-toxic level (Israr et al., 2011; Štefanić et al., 2018; Du et al., 2020). In the past two decades, many studies have estimated the direct link between the oxidative stress in metal toxicity and metal-tolerant plants (Boominathan and Doran, 2003; Chiang et al., 2006). A large proportion of studies have indicated that metal tolerant plants were linked to superior constitutive antioxidative defense (Srivastava and Doran, 2005; Chiang et al., 2006; Nie et al., 2016). Although great progress has been made in supporting the HM toxicity to plant photosynthesis and its redox balance, the effects of HM stress on photosynthetic performance varied depending on the plant species, metal ion and concentration. Meanwhile, these available data provide a restricted view on single metal contamination or herbaceous plants (Mobin and Khan, 2007; Wali et al., 2016). Therefore, the photosynthesis and redox responses of trees to HM tailing stress still need to be studied further.

Melia azedarach is a fast-growing, deciduous broad-leaved tree species and is widely distributed in the southern regions of China. It is mainly planted for reforestation as a useful timber production species or as an ornamental plant. *Ligustrum lucidum* is a commonly-seen evergreen broad-leaved tree species in South China. This species is often planted as an ornamental tree in the urban. Moreover, both *M. azedarach* and *L. lucidum* are native plants in the southern regions of China, Frérot et al. (2006) pointed out that native plants could be a useful option to phytoremediation because native plants are better adapted to local climate conditions than plants introduced from other environments, and they were previously found to have high tolerance in Cd or Mn contaminated soils (Trikshiqi and Rexha, 2015; Su et al., 2017; Liang et al., 2019). However, the metal toxicity manifestations and mechanisms behind tolerance need further investigation, so the specific goals of this study were: 1) to investigate the contributions of Gs, Gm, and biochemical component respectively to the photosynthesis reduction in two

tested plants by photosynthesis limitation analysis, 2) to identify the impact of Pb–Zn stress on the whole photosynthetic electron flow chain from PSII to PSI and the state of PSI, 3) to explore the tolerant mechanisms of both trees to Pb–Zn tailing stress in terms of the redox responses of photosystems and antioxidative enzymes. Based on the above studies, the differences of tolerance between *M. azedarach* and *L. lucidum* were discussed. Results could provide a theoretical basis for selecting and breeding the resistant trees species grown in Pb–Zn polluted environments.

MATERIALS AND METHODS

The Physicochemical Properties of Pb–Zn Tailings and Experimental Soil

The study was conducted in the Central South University of Forestry and Technology (CSUFT), Changsha City, Hunan Province, China (28°8′12″N, 112°59′36″E). The Pb–Zn mine tailing samples were collected from a Pb–Zn mining site in Suxian district, Chenzhou City, Hunan Province, China (25°30′38″–25°00′19″N, 112°16′41″–112°53′23″E). The soil samples were collected from the top soil (5–20 cm) in a garden field of CSUFT campus. Both Pb–Zn mine tailing samples and top soil samples were air-dried at room temperature. The large debris, stones, and pebbles were manually removed before being applied to the pot experiment. The soil pH value, soil total carbon (TC), total nitrogen (TN), total phosphorus (TP), and soil heavy metal content were measured in laboratory according to Bao (2000), the basic physicochemical properties of soil were as follows: pH 4.95, total C 5.82 g kg^{-1}, total N 0.33 g kg^{-1}, total P 0.16 g kg^{-1}, Pb 0.002 g kg^{-1}, Zn 0.003 g kg^{-1}. The properties of Pb–Zn mine tailing samples were determined: pH 3.89, total C 13.89 g kg^{-1}, total N 1.25 g kg^{-1}, P 0.82 g kg^{-1}, Pb 8.92 g kg^{-1}, Zn 14.41 g kg^{-1}.

Plant Seedlings

Two-year-old young plants of *M. azedarach* (mean tree height: ~73.5 cm, mean stem base diameter: ~0.6 cm) and *L. lucidum* (mean tree height: ~130.0 cm, mean stem base diameter: ~0.9 cm) were purchased from a local nursery.

Experimental Design

Pb–Zn mine tailings represent a poor spoil substrate characterized by high contents of Pb and Zn, low levels of organic nutrients, and poor physical structure and water retention capacity (Meeinkuirt et al., 2012); few plants can survive in such harsh environmental condition. Mixing mine tailings with garden soil helps decrease the bioavailability of metals and improves mine tailing structure and ultimately upgrades the physical properties and nutrient status of mine tailings. Moreover, this method has been commonly used in many studies of phytoremediation in mine tailing (Chen et al., 2015; Han et al., 2016; Tang et al., 2019). In the present study, four treatments were set up in the pot experiment with different weighted proportions of Pb–Zn mine tailings and garden soils. Each pot contained 10 kg mixed soils. The four treatments were: (1) 90% garden soils + 10% Pb–Zn mine tailings (designed as L1, the 10 kg mixed soils were 9 kg garden soil and 1 kg mine tailings, the same as below); (2) 75% garden soils + 25% Pb–Zn mine tailings (L2); (3) 50% garden soils + 50% Pb–Zn mine tailings (L3), and (4) 100% garden soils + 0% Pb–Zn mine tailings as the control (C). The Pb–Zn mine tailings and garden soils were completely mixed and then the *M. azedarach* and *L. lucidum* young plants were transplanted into the pots with one plant per pot. Each treatment was replicated six times. The temperatures of the greenhouse were set at 30/25°C (day temperature for 10 h and night temperature for 14 h), and relative humidity was 65/85%. During the study period, each pot was supplied with equal quantity of pure water every 1 to 2 days until the young plants were harvested. Both trees were measured for all physiological parameters after growing for 425 days (from June 15th, 2017 to September 13th, 2018) in Pb–Zn tailing treatments.

Relative Growth Rate (RGR)

Plant biomass was measured using a harvesting method. The plant was divided into leaves, stem, and root components; the fresh weights of each component were measured by using an electronic balance and then dried at 70°C until constant weight was reached. The dry weight (DW) of each component was determined by using an electronic balance. Six individual plants were selected for biomass measurement for each of *M. azedarach* and *L. lucidum* species at the beginning of the treatment, respectively, as initial dry weight (DW). The biomass of each component was determined as initial dry weight (DW). After 425 days of treatment (from June 15th, 2017 to September 13th, 2018), all examined plants were harvested and the biomass was measured as final DW. The determination of relative growth rate (RGR) is based on the method of Environment Canada (2007) guidelines as follows:

$$RGR = (ln \quad X_j - \ln X_i)/(t_j - t_i);$$

where X_i and X_j represent the values of final DW and initial DW, respectively; t_j and t_i represent initial time and final time, respectively.

Gas Exchange Measurements

Three new, similar size and fully expanded leaves per plant were chosen for the measurements of photosynthesis for each treatment. The leaf gas exchange and Chl fluorescence were measured by using an open gas exchange system (LI-COR 6400XT, Lincoln, USA) at the same time with an integrated Chl fluorescence chamber head in the morning (8:00–10:00 am). For all measurements, the following conditions were set up: leaf temperature of 25–32°C, PAR of 1,000 μmol (photon) m^{-2} s^{-1}, and vapor pressure deficit (VPD) of 2.0 ± 0.2 kPa.

For developing the relationships between leaf photosynthesis and intercellular CO_2 concentrations (A–Ci curves), the steady-state rates of leaf maximum net photosynthesis rate (P_n, μmol m^{-2} s^{-1}), stomatal conductance (Gs, mol m^{-2} s^{-1}) and intercellular CO_2 concentration (Ci, μmol m^{-2} s^{-1}) were measured. The A–Ci curves were developed by measuring P_n at 15 reference CO_2 concentrations: 400, 300, 250, 200, 150, 100, 50, 25, 0, 400, 600, 800, 1,000, 1,200, 1,400 μmol mol^{-1} as described by Centritto et al.

(2003). The maximum carboxylation rate allowed by Rubisco (V_{cmax}), day respiration (R_d), and electron transfer rate of photosynthesis based on NADPH requirement (J_{max}) were estimated based on the modeling methods (Farquhar et al., 1980; Sharkey et al., 2007).

Mesophyll conductance to CO_2 (Gm) was calculated by using 'variable J method' (Harley et al., 1992; Sagardoy et al., 2010) as:

$$Gm = P_n/(Ci)(\Gamma*(J_{flu} + 8(P_n + R_d))/((J_{flu})4(P_n + R_d)) \quad (1)$$

where, P_n and Ci were obtained from gas exchange measurements under saturating light, $\Gamma*$ was the CO_2 concentration at the compensation point in the absence of mitochondrial respiration and was obtained according to Bernacchi et al. (2002), R_d was calculated based on the A–Ci curve on the same leaf according to Pinelli and Loreto (2003).

J_{flu} represented the rate of electron transport and was calculated as:

$$J_{flu} = 0.5 \cdot \varphi PSII \cdot \alpha \cdot PPFD \quad (2)$$

where, α was total leaf absorbance in the visible light range (taken as 0.85, Grassi and Magnani, 2005), 0.5 was a factor to account for the distribution of light between the two photosystems (Laisk and Loreto, 1996). The actual chloroplastic CO_2 concentration (Cc) was calculated from the g_m value as Cc = Ci – (P_n/Gm) (Harley et al., 1992).

Photosynthesis Limitation Analysis

The inhibition of Pb–Zn stress on plant photosynthesis was further assessed based on the contribution made by various functional components to the photosynthetic limitations (Sagardoy et al., 2010). The functional components were stomatal (SL), mesophyll conductance (MCL), and leaf biochemical characteristics (BL). The relative contributions of these functional components to the photosynthesis limitations were evaluated when compared with a reference status in which the photosynthesis limitations were ignorable, and the Gs, Gm, and V_{cmax} were at their maximum. In this study, the corresponding values of Gs, Gm, and V_{cmax} taken from C treatments were as reference values; thus the photosynthesis limitations were set to 0.

The Kinetics of Prompt Fluorescence and Modulated 820 nm Reflection

Fast chlorophyll a fluorescence was measured by using M-PEA (Multifunctional Plant Efficiency Analyser, Hansatech Instrument, UK). After 1 h dark adaptation using dark adaptation clips, leaves were exposed to a pulse of saturating red light (5,000 μmol m^{-2} s^{-1}, peak at 625 nm, duration from 50 μs to 2 s, records of 128 points), and the measurements were carried out during a period of 8:30–11:00 am. The OJIP transient was analyzed based on the JIP test (Strasser et al., 2004). The values of fluorescence intensity from the original measurements were used in this study: fluorescence intensity at 20 μs (at the O step, considering as the minimum fluorescence, F_O); 300 μs ($F_{300\mu s}$) used for calculation of the initial slope of the relative variable fluorescence kinetics; 2 ms (at the J step, F_J); 30 ms (at the I step, F_I), and the P step (considering as the maximum fluorescence, F_m). The description and calculation of standardization formula of OJIP transients and formula of parameters were listed in **Table 1**.

Modulated 820 nm reflection was also expressed as MR/MR_O. The value of MR and MR_O were determined by the method of Zhou et al. (2019). The PSI redox was denoted by V_{PSI} (maximum PSI oxidation rate) and $V_{PSII–PSI}$ (maximum PSI reduction rate, respectively, and were obtained according to Gao et al. (2014).

Evaluation of Chlorophyll and Carotenoid Contents

Leaf chlorophylls and carotenoid content were extracted using 95% ethanol and then placed in the dark for at least 72 h at 4°C. The extracts were measured at wavelengths of 665, 649, and 470 nm spectrophotometrically and was then calculated as milligram per gram of fresh weight (Ji et al., 2018).

Assay of Superoxide Anion (O_2^-) Production Rate, H_2O_2 Content, and Malondialdehyde (MDA)

The O_2^- production rate was measured using a reagent kit (Beijing Solarbio Science and Technology, China). H_2O_2 content was measured using the method of Okuda et al. (1991). The MDA level was assayed as a thiobarbituric acid reactive substance according to the method of Dhindsa et al. (1981). A 0.25 g fresh leaf sample was homogenized; supernatant was collected and measured at the wave length of 532, 600, and 450 nm using a UV/visible spectrophotometer.

Estimation of Proline and Antioxidative Enzymes

Proline content was determined using Pure Pro as a standard (Gao, 2006). A 0.1 g fresh leaf sample was homogenized with 5 ml of 3% aqueous sulfosalicylic acid and was then extracted in a boiling bath.

For determination of SOD, POD, and CAT, a 0.3 g fresh leaf sample was grounded in 3 ml extraction buffer containing 25 mM Hepes, 2% polyvinyl-pyrrolidone (PVP), 0.2 mM EDTA, and 2 mM ascorbate (pH 7.8) and was centrifuged at 12,000 g for 20 min at 4°C. The supernatants were collected for enzyme analysis.

SOD activity was determined according to Giannopolitis and Ries (1977). The 3 ml reaction mixture contained 0.05 M phosphate buffer solution (pH 7.8), 0.06 M Riboflavin, 0.195 M Met, 0.003 M EDTA, 1.125 mM NBT, and 0.2 ml enzyme supernatants. The measurements were performed at 25°C. The tested samples were incubated for 10–20 min under 10,000 lx irradiance; inhibition rate of nitro blue tetrazolium (NBT) reached to 50% represented one unit of SOD activity as by spectrophotometer at 560 nm.

POD activity was assessed as in Beffa et al. (1990). The reaction mixture contained 0.1 M sodium-acetic buffer (pH 5.0), 0.25% (w/v) guaiacol, 0.75% H_2O_2, and 0.05 ml enzyme supernatants. One unit of POD activity was represented as an increase of 0.01 ΔOD value a minute at 470 nm.

CAT activity was determined according to Aebi (1984). The reaction mixture contained 0.05 M phosphate buffer (pH 7.0)

TABLE 1 | Formulae and definitions the technical data of the OJIP curves, the selected JIP-test parameters and the selected PF parameters used in this study.

Technical fluorescence	
F_t	Fluorescence at time t after onset of actinic illumination
$F_O \cong F_{20\mu s}$ or $F_{50\mu s}$	Minimal fluorescence, when all PSII RCs are open
$F_K = F_{300\mu s}$	Fluorescence intensity at the K-step (300 μs) of OJIP
$F_J = F_{20ms}$	Fluorescence intensity at the J-step (2 ms) of OJIP
$F_I = F_{30ms}$	Fluorescence intensity at the I-step (30 ms) of OJIP
$F_P(=F_M)$	Maximal recorded fluorescence intensity, at the peak P of OJIP
N	the turnover number of QA reduction events
$F_v = F_t - F_O$	Variable fluorescence at time t
$F_V = F_M - F_O$	Maximal variable fluorescence
$V_I = (F_M - F_I)/(F_M - F_O)$	Relative variable fluorescence at time t
$V_K = (F_K - F_O)/(F_M - F_O)$	Relative variable fluorescence at the K-step
$V_J = (F_J - F_O)/(F_M - F_O)$	Relative variable fluorescence at the J-step
$W_K = W_{300\mu s} = (F_{300\mu s} - F_O)/(F_J - F_O)$	Relative variable fluorescence at the K-step to the amplitude F_J-F_O
$\varphi_{Po} = PHI(P_0) = TR_0/ABS = 1 - F_O/F_M$	Maximum quantum yield for primary photochemistry
$\psi_{Eo} = PSI_0 = ET_0/TR_0 = (1 - V_J)$	Probability that an electron moves further than QA^-
$\varphi_{Eo} = PHI(E_0) = ET_0/ABS = (1 - F_O/F_M)/(1 - V_J)$	Quantum yield for electron transport (ET)
$\varphi_{Ro} = RE_0/ABS = \varphi_{Po} \times \psi_{Eo} \times \delta_{Ro} = \varphi_{Po} \times (1 - V_I)$	Quantum yield for reduction of the end electron acceptors on the PSI acceptor side (RE)
$\delta_{Ro} = RE_0/ET_0 = (1 - V_I)/(1 - V_J)$	Probability that an electron is transported from the reduced intersystem electron acceptors to the final electron acceptors of PSI (RE)
ABS/CS = CH1/CS	Absorption flux per CS
$RC/CS = \varphi_{Po} \times (V_J/M_0) \times (ABS/CS)$	Q_A-reducing RCs per CS
$PI_{ABS} = \frac{\gamma RC}{1-\gamma RC} \times \frac{\varphi Po}{1-\varphi Po} \times \frac{\varphi Eo}{1-\varphi Eo}$	Performance index (potential) for energy conservation from photons absorbed by PSII to the reduction of intersystem electron acceptors
$\Delta V_{IP} = 1 - V_I$	Amplitude of the I to P phase of the OJIP fluorescence transient (associated with PSI reaction center content).
Abbreviations	
P_n	net photosynthetic rate
Gs	stomatal conductance
Ci	intercellular CO_2 concentration
Gm	mesophyll conductance to CO_2
Rd	day respiration
Cc	chloroplastic CO_2 concentration
V_{cmax}	Maximum carboxylation rate allowed by Rubisco
J_{max}	rate of photosynthetic electron transport based on NADPH requirement
SL	stomatal conductance
MCL	mesophyll conductance
BL	biochemical limitation
MDA	malondialdehyde
SOD	superoxide dismutase
POD	peroxidase
CAT	Catalase

and 0.45 M H_2O_2 and 0.2 ml enzyme supernatants. One unit of CAT activity was represented as decrease of ΔOD value a minute at 240 nm. The measurement for each antioxidative enzyme was repeated three times.

Assay of Leaf Total Rubisco Activity

Ribulose-1, 5-bisphosphate carboxylase/oxygenase (Rubisco) of leaves from the tested plants was assayed according to the method of Chen et al. (2005). After centrifugation at 13,000 $r{\cdot}min^{-1}$ 40 s at 2°C, the supernatant was used immediately for assays of Rubisco activity (Jiang et al., 2008).

Total Metal Content

For the determination of the metal contents in plant, the different dried plant components were powdered and passed through an 80-mesh sieve. About 0.1 g of plant material was digested with 1 ml of HNO_3 and H_2O_2 (8:2, v/v). Then, the tube with plant material was on the block at 200°C for 0.75–1 h. The residue was taken up in 10 ml of demineralized water. The concentrations of Pb and Zn were determined by atomic absorption spectrophotometry (AA-6800, Shimadzu, Kyoto, Japan) (Huang et al., 2019). The measurement for each sample was repeated six times, and the mean value was calculated.

The metal translocation factor (TF) in the leaves was represented as the metal concentration ratio of plant leaves and stems to roots (Han et al., 2016).

Statistical Analyses

Two-way analysis of variance (ANOVA) was performed on the data using SPSS (20.0). Differences among the eight treatment combinations (two species × four Pb–Zn mine tailing treatments) were analyzed by two-way analysis of variance; eight means were separated by Duncan's new multiple range test at $P < 0.05$ level. Data were presented as means ± SD (n = 6). The principal component analysis (PCA) used CANOCO version 5.0.

RESULTS

RGR, Pb/Zn Contents in Roots, Stems, and Leaves

As Pb–Zn tailing portions increased, RGR of *M. azedarach* and *L. lucidum* was decreased progressively compared with the control group ($P < 0.05$) (**Table 2**), the RGR values were reduced by 10–90% and 6–70% in *M. azedarach* and *L. lucidum*, respectively, in Pb–Zn treatments when compared with the C plants (**Table 2**). The concentrations of Pb and Zn in the leaves, stems, and roots increased with the increase of the proportion of Pb–Zn tailings in both tested plants compared to the C (**Table 2**). The Pb and Zn concentrations were significantly higher in the roots than in the leaves and stems. The Pb and Zn concentrations showed as Zn > Pb in the leaves, stems, and roots in all Pb–Zn tailing treatments. TFs of Pb and Zn were higher in *M. azedarach* than those in *L. lucidum*.

TABLE 2 | Relative growth rate (RGR), Pb and Zn concentrations and translocation coefficient of *M. azedarach* and *L. lucidum* grown in soil mixed with different proportions of Pb–Zn mine tailings.

		RGR	Pb content				Zn content			
			Root	Leaf	Stem	TF	Root	Leaf	Stem	TF
M. azedar-ach	C	0.010 ± 0.002a	0.57 ± 0.04a	0.31 ± 0.06a	0.15 ± 0.05a	0.80 ± 0.27a	27.32 ± 1.98a	30.36 ± 1.56a	31.44 ± 0.91a	2.26 ± 0.22a
	L1	0.009 ± 0.004a	15.93 ± 0.41b	9.68 ± 0.78b	8.01 ± 0.35b	1.11 ± 0.31b	49.12 ± 2.32b	70.5 ± 3.34b	33.88 ± 1.05a	2.13 ± 0.35a
	L2	0.005 ± 0.003b	43.96 ± 2.18c	26.08 ± 2.56c	13.67 ± 3.32c	0.90 ± 0.16a	101.49 ± 3.22c	126.41 ± 4.78c	41.81 ± 2.25b	1.66 ± 0.27b
	L3	0.001 ± 0.000c	105.13 ± 6.83d	50.98 ± 1.45d	16.39 ± 0.41c	0.65 ± 0.22a	236.14 ± 7.63d	177.88 ± 8.34d	62.15 ± 3.04c	1.01 ± 0.18c
L. lucidu-m	C	0.018 ± 0.002a	0.31 ± 0.04a	0.41 ± 0.04a	0.22 ± 0.02a	2.02 ± 0.11a	24.15 ± 2.02a	28.46 ± 0.57a	24.36 ± 1.12a	2.19 ± 0.33a
L1	0.017 ± 0.001b	20.84 ± 1.22b	5.48 ± 0.63b	5.41 ± 0.22b	0.52 ± 0.09b	69.51 ± 4.41b	50.32 ± 4.32b	33.12 ± 0.76b	1.20 ± 0.25b	
L2	0.009 ± 0.002c	59.78 ± 3.54c	15.64 ± 1.15c	8.46 ± 0.76c	0.40 ± 0.12b	158.45 ± 5.67c	78.16 ± 4.09c	36.39 ± 1.77b	0.72 ± 0.21b	
L3	0.005 ± 0.003d	141.04 ± 4.32d	36.75 ± 1.93d	9.13 ± 0.55c	0.33 ± 0.04b	288.12 ± 8.91d	99.65 ± 3.88d	51.12 ± 2.09c	0.53 ± 0.11c	

TF = the metal concentration ratio of plant leaves and stems to roots. Data are means ± SE, n = 6. Values with different letters within the same column indicate significant differences at the p < 0.05 level between Pb–Zn treatments. C: 100% garden soil, L1: 90% garden soil + 10% Pb–Zn tailings, L2: 75% garden soil + 25% Pb–Zn tailings, L3: 50% garden soil + 50% Pb–Zn tailings.

Pigment Contents

The photosynthetic pigment contents of the two tested plants were found to decline with increasing Pb–Zn tailing portions (**Figures 1A–D**). A significant reduction in chlorophylls a, b, and total chlorophyll in the two tested plants was observed under Pb–Zn tailing stress as compared to the C, respectively. Carotenoid content was notably affected by Pb–Zn tailing stress when the Pb–Zn treatment exceeded a portion of 10%. Compared with *L. lucidum*, *M. azedarach* showed a faster increase and a greater extent of chlorophylls a, b, total chlorophyll, and carotenoid content. When compared to the C groups, Chl a decreased by a range of 18 to 50%, Chl b from 9 to 35%, total chlorophyll from 16 to 46%, and the carotenoids from 5 to 37% in *L. lucidum* in L1–L3 treatments. The corresponding values decreased in *M. azedarach* from 4to 42% in Chl a, from 5 to 21% in Chl b, from 5 to 37% in total chlorophyll, and from 3 to 34% in carotenoids.

Gas Exchange

The Pb–Zn tailing treatments had an inhibitory effect on Pn, Gs, Gm, V_{cmax}, J_{max}, and Rubisco activity, but had promotion effect on Ci and Cc in both examined plants (**Figure 2**). Pn, V_{cmax}, J_{max} significantly decreased after Pb–Zn mine tailing treatment. The Gm of the leaves from the two plants gradually decreased with the increase of Pb–Zn tailing portions. For *M. azedarach*, Gs showed a significant difference between C and L1 treatments and then gradually decreased when the plants were grown in L2 treatments, and eventually reached the minimum value at L3 treatments. In *L. lucidum*, Gs was decreased slightly as Pb–Zn tailing portions increased. Both plants exhibited the similar tendency in Ci and Cc as Pb–Zn tailing portions increased. Ci and Cc decreased slightly when the plants were in L1 treatments and then significantly increased in L2 and L3 treatments ($P < 0.05$), but the change of Ci was higher in *L. lucidum* (increased from −5 to 58%) than in *M. azedarach* (increased from −4 to 5%). The decrease of P_n, Gm, V_{cmax}, and J_{max} in *M. azedarach* showed a greater extent than that in *L. lucidum*. When compared to the C groups, the Pn decreased by a range of 12 to 56%, the Gm from 7 to 18%, the V_{cmax} from 9 to 43%, the J_{max} from 19 to 64%, and the Rubisco activity from 10 to 52% in *L. lucidum* in L1–L3 treatments. The corresponding values decreased in *M. azedarach* from 31 to 67% in Pn, from 10 to 28% in Gm, from 16 to 59% in V_{cmax}, from 21 to 72% in J_{max}, and from 31 to 62% in the Rubisco activity.

Under Pb–Zn tailing treatments, biochemical limitations (BLs) increased in the two tested plants. The BL values of *M. azedarach* increased 12, 34, and 53% in the L1, L2, and L3 treatments compared to the C, respectively (**Table 3**). The corresponding values increased 6, 23, and 36% in L1, L2, and L3 treatments in *L. lucidum*, respectively. The stomatal conductance limitation (SL) and the mesophyll conductance (MCL) of leaves in both trees increased slightly under Pb–Zn treatments. The SL values increased 4–6% and the MCL values increased 0.4–0.8% for *M. azedarach* and *L. lucidum* when compared to C.

Prompt Fluorescence OJIP Transient Analysis

The Pb–Zn stress had a considerable effect on fluorescent OJIP transients in two tested plants (**Figure 3**). The F_o values were

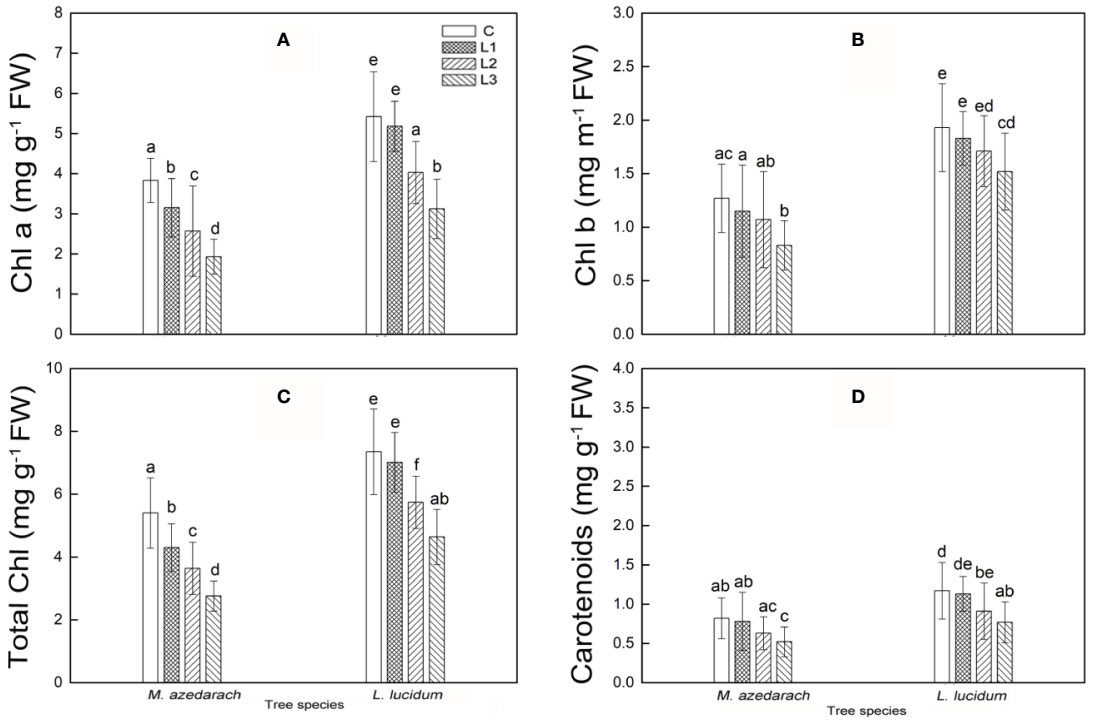

FIGURE 1 | Chlorophyll a **(A)**, chlorophyll b **(B)**, total chlorophyll **(C)** and carotenoids **(D)** in leaves of *M. azedarach* and *L. lucidum* grown in soil mixed with different proportions of Pb–Zn mine tailings. C (control), L1, L2, and L3 represent 100% garden soil, 90% garden soil + 10% Pb–Zn tailings, 75% garden soil + 25% Pb–Zn tailings, 50% garden soil + 50% Pb–Zn tailings, respectively. Different letters above the bars indicate a significant difference at $P < 0.05$. Values are means of n = 6; bar indicates standard error.

significantly reduced under Pb–Zn treatments in *M. azedarach* compared to the C (**Figure 3A**, inset). However, the F_o values of *L. lucidum* had no significant increase under Pb–Zn tailing treatments compared to the C (**Figure 3B**, inset). Three Pb–Zn tailing treatments did not affect W_k in *L. lucidum* compared to the C (**Figure 4A**). In *M. azedarach*, W_k was similar for both C and L1 treatments and significantly increased in L2 and L3 treatments (**Figure 4A**). Pb–Zn stress treatments significantly decreased performance index (PIabs) in *M. azedarach* and *L. lucidum* (**Figure 4B**) but distinctly increased the turnover number of Q_A reduction events (N) and absorption flux (ABS/RC) (**Figures 4F, G**). Meanwhile, RC/CS_O, TR_O/ABS, and ET_O/TR_O were decreased dramatically by Pb–Zn stress (**Figures 4C–E**).

The value of φR_o, δR_o and ΔV_{IP} significantly decreased in *M. azedarach* and *L. lucidum* as Pb–Zn tailing portions increased (**Figures 4H–J**). When compared to the C groups, the φR_o decreased by 21, 34, and 40%, the δR_o decreased by 32, 33, and 47%, and the ΔV_{IP} decreased by 18, 33, and 53% in *M. azedarach* in L1, L2, and L3 treatments, respectively. The corresponding values decreased 19, 24, and 36% in φR_o, 17, 30 and 35 in δR_o, 17, 26, and 37% in ΔV_{IP} in *L. lucidum*.

MR/MR$_O$ Transient Analysis

After Pb–Zn tailing treatments, the shape of the MR/MR_O kinetics was obviously changed in the two tested plants. The lowest points represented a turning point of PSI oxidation state (**Figure 5**). When compared to the C, the lowest points on the reflection curve of both tested plants increased with rising Pb–Zn tailing portions. The V_{PSI} and $V_{PSII-PSI}$ of both tested plants declined significantly with the rising Pb–Zn tailing portions (**Table 4**). V_{PSI} and $V_{PSII-PSI}$ of both tested plants significantly decreased in the treated groups than in the C groups. Compared with *L. lucidum*, *M. azedarach* showed a greater decrease of V_{PSI} and $V_{PSII-PSI}$.

PI$_{abs}$, ΔV_{IP} in Relation to V$_{cmax}$

A significant positive relationship of PI_{abs}, ΔV_{IP} and V_{cmax} was observed in both tested plants under Pb–Zn mine tailing treatments (**Figure 6**). As V_{cmax} decreased, PI_{abs}, ΔV_{IP} decreased linearly in *M. azedarach* and *L. lucidum*, respectively.

O_2^- Production Rate, H_2O_2, MDA and Proline Content in Leaves

With an increase of Pb–Zn mine tailing portions, the O_2^- production rate, H_2O_2, and MDA contents of two tested plant leaves increased notably (**Figures 7A, C, D**). Compared with *L. lucidum*, *M. azedarach* showed a faster increase and a greater extent O_2^- production rate, H_2O_2, and MDA contents. The proline content in *M. azedarach* and *L. lucidum* reached the peak at L2 treatments (**Figure 7B**), where the proline content was 1.96 and 1.36 times higher than that in the C treatments,

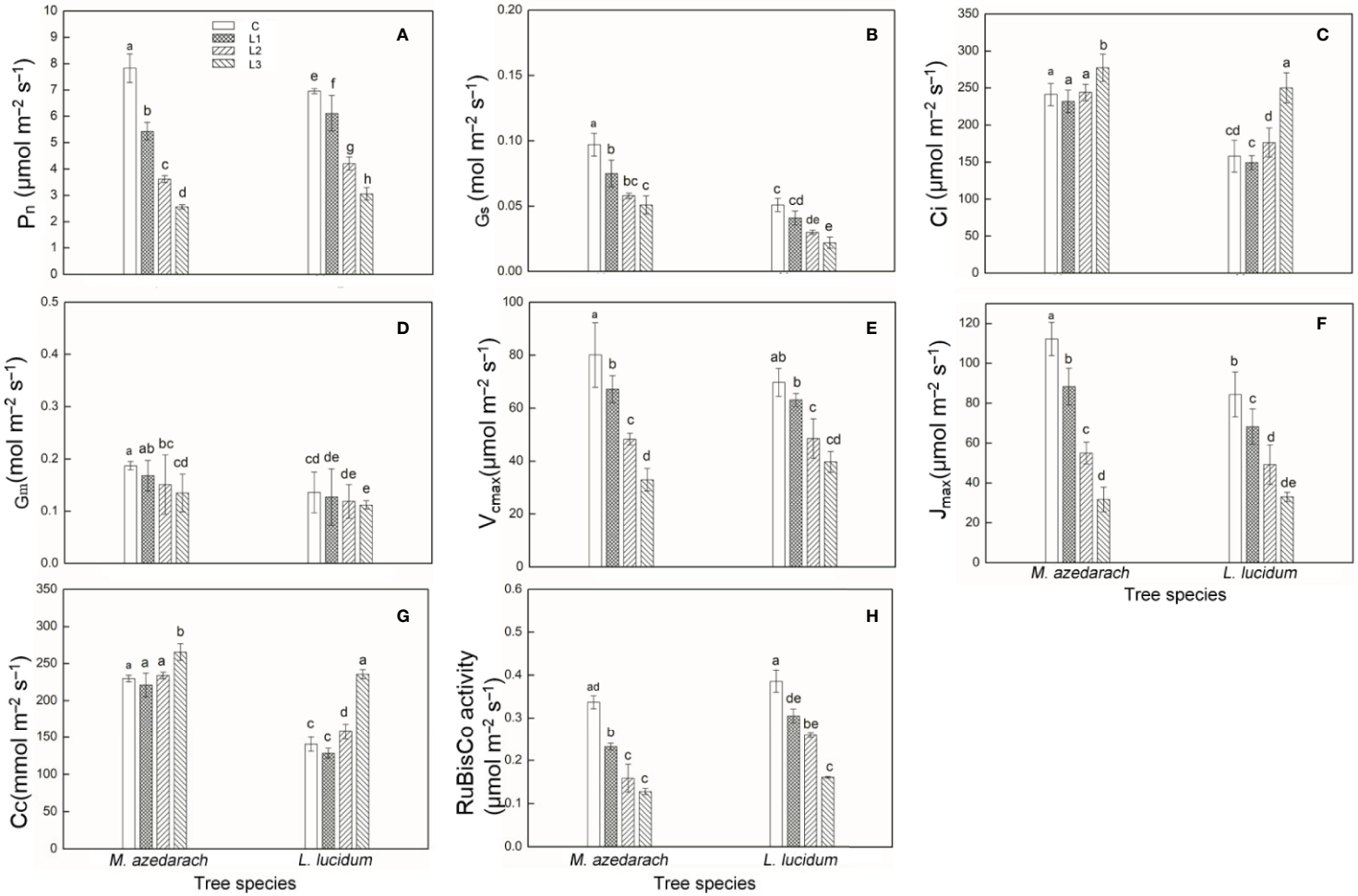

FIGURE 2 | Photosynthetic parameters measured with a Li-6400 gas exchange system and rubisco activity in *M. azedarach* and *L. lucidum* grown in soil mixed with different proportions of Pb–Zn mine tailings. **(A)** Pn, net photosynthetic rate; **(B)** Gs, stomatal conductance; **(C)** Ci, intercellular CO_2 concentration; **(D)** Gm, mesophyll conductance to CO_2; **(E)** V_{cmax}, maximum carboxylation rate allowed by Rubisco; **(F)** J_{max}, rate of photosynthetic electron transport based on NADPH requirement; **(G)** Cc, chloroplastic CO2 concentration; **(H)** Rubisco activity. C (control), L1, L2, and L3 represent 100% garden soil, 90% garden soil + 10% Pb–Zn tailings, 75% garden soil + 25% Pb–Zn tailings, 50% garden soil + 50% Pb–Zn tailings, respectively. Different letters above the bars indicate a significant difference at $P < 0.05$. Values are means of $n = 6$; bar indicates standard error.

TABLE 3 | Photosynthesis limitation parameters (%) in *M. azedarach* and *L. lucidum* grown in soil mixed with different proportions of Pb–Zn mine tailings.

	C	Pb–Zn tailings treatments		
		L1	L2	L3
M. azedarach				
SL	0.0%	5.1%	5.6%	4.0%
MCL	0.0%	0.5%	0.5%	0.8%
BL	0.0%	12.2%	33.6%	53.1%
L. lucidum				
SL	0.0%	5.0%	6.0%	6.4%
MCL	0.0%	0.4%	0.5%	0.4%
BL	0.0%	5.8%	23.1%	35.9%

Data are means ± SE, n = 6. The control (C) was taken as a reference, for which all limitations were set to 0. SL: stomatal conductance limitation, MCL: mesophyll conductance, BL: biochemical limitations. L1: 90% garden soil + 10% Pb–Zn tailings, L2: 75% garden soil + 25% Pb–Zn tailings, L3: 50% garden soil + 50% Pb–Zn tailings.

respectively. Under L3 treatments, the proline content in *M. azedarach* and *L. lucidum* decreased by 16 and 13% of that in the C, respectively.

Antioxidant Enzyme Activity in Leaves

The SOD, POD, and CAT displayed similar trends in activity in both tested trees with the increase of Pb–Zn mine tailing portions (**Figures 8A–C**). Compared with the C, the activities of SOD and POD in both tested trees significantly increased under L1 and L2 treatments and decreased under L3 treatment. The CAT activity in both tested trees under all Pb–Zn treatments was significantly higher than that in the C plants. Notably, the activities of SOD, POD, and CAT in *L. lucidum* were significantly higher than that in *M. azedarach* under all Pb–Zn mine tailing treatments.

Principal Component Analysis

PCA was used to understand Pb–Zn tailings affecting the photosynthetic characteristics including RGR, PSII performance, PSI content, net photosynthesis rates (Pn), and the antioxidative enzymes of leaves in both trees (**Figure 9**). The first two components comprised 90.0% (50.3% for PC1 and 39.7% for PC2), 91.4% (62.9% for PC1 and 28.5% for PC2), and 90.9% (36.7% for PC1 and 54.2% for PC2) of the total variations in L1, L2, and L3 treatments, respectively. Under L1 and L2 treatments, PIabs, ΔV_{IP}, and Pn were the most influential in the PC1; and SOD, POD and CAT in the PC2. Under L3 treatments, SOD, POD, and CAT were the most influential in the PC1, and PIabs and ΔV_{IP} in the PC2. Evidently, two tested plans were more closely to photosynthetic parameters (PIabs, ΔV_{IP}, and Pn) than to antioxidative enzymes (SOD, POD and CAT) under L1 and L2 treatments, but were more closely to antioxidative enzymes than to photosynthetic parameters under L3 treatment. In addition, RGR was positively related to the photosynthetic parameters in the tested plants.

DISCUSSION

The Reduction of Plant Growth Is Attributed to the Depression of Photosynthesis

When plants were grown in Pb–Zn contaminated soils, plant growth and development were retarded and eventually the biomass production decreased (Ha et al., 2011; Han et al., 2013). In this study, the RGR values for the two tested trees decreased under Pb–Zn treatments (**Table 2**). It was well known that plant biomass productivity was dependent on the photosynthetic assimilating accumulation which provided energy and carbon sources (Liu et al., 2017). A positive correlation was found between Pn and RGR in this study (**Figure 9**), suggesting the photosynthetic processes were inhibited by Pb–Zn stress in the tested tree species.

The Photosynthesis Limitation Is Mainly Attributed to the Biochemical Limitation

A significant decrease of gas exchange parameters was observed in the Pb–Zn treated plants (**Figure 2**). Photosynthesis limitations might be derived from different physiological

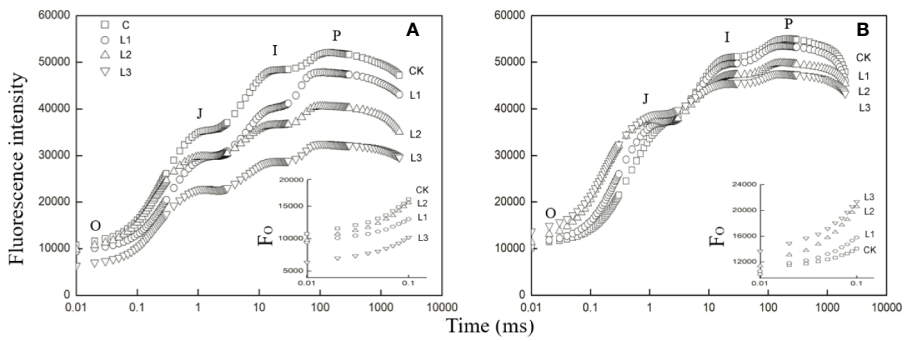

FIGURE 3 | Fast induction curves of chlorophyll fluorescence (OJIP) in *M. azedarach* **(A)** and *L. lucidum* **(B)** grown in soil mixed with different proportions of Pb–Zn mine tailings. The letters O, J, I, and P refer to the selected time points used by the JIP-test for the calculation of structural and functional parameters. The used signals are: the fluorescence intensity at $F_O \cong F_{20\mu s}$ or $F_{50\mu s}$; at 3 ms = F_J; and at 30 ms = F_I; the maximal fluorescence intensity, $F_P = F_M$. C (control); L1, L2, and L3 represent 100% garden soil, 90% garden soil + 10% Pb–Zn tailings, 75% garden soil + 25% Pb–Zn tailings, 50% garden soil + 50% Pb–Zn tailings, respectively. In the insets of the two panels, the F_O of the fluorescence rise is compared between measurements on control and Pb–Zn treated leaves.

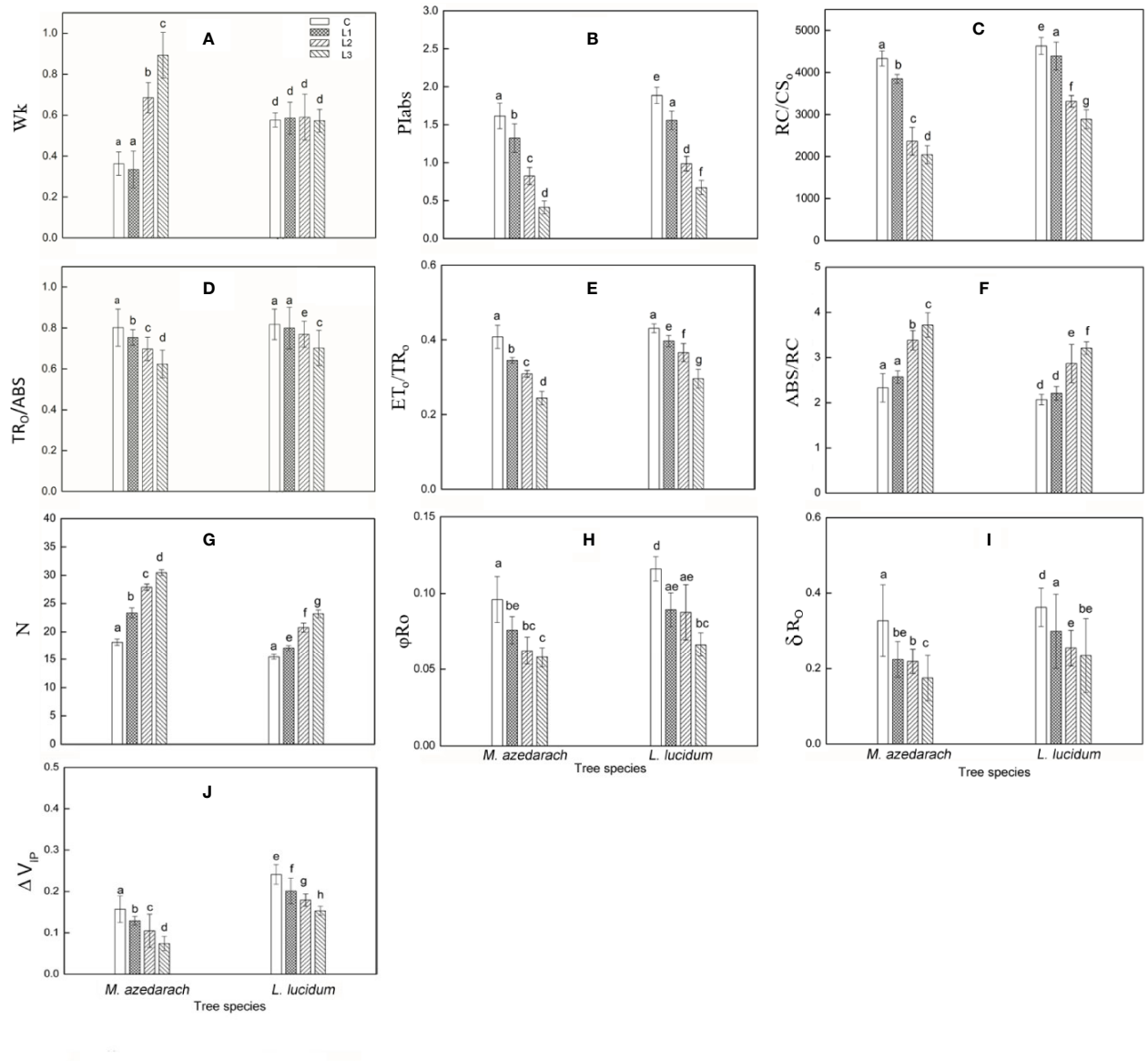

FIGURE 4 | Parameters derived from OJIP transients of *M. azedarach* and *L. lucidum* grown in soil mixed with different proportions of Pb–Zn mine tailings. **(A)** W_K, relative variable fluorescence at the K-step to the amplitude F_J–F_O; **(B)** PI_{ABS}, performance index (potential) for energy conservation from photons absorbed by PSII to the reduction of intersystem electron acceptors; **(C)** RC/CS_O, the density of PSII reaction center (RC) per excited cross-section (at t = 0); **(D)** TR_O/ABS, maximum quantum yield for primary photochemistry; **(E)** ET_O/TR_O, probability that an electron moves further than QA^-; **(F)** ABS/CS, absorption flux per unit area; **(G)** N, the turnover number of Q_A reduction events; **(H)** φ_{Ro}, quantum yield for reduction of the end electron acceptors on the PSI acceptor side (RE); **(I)** δ_{Ro}, probability that an electron is transported from the reduced intersystem electron acceptors to the final electron acceptors of PSI (RE); **(J)** ΔV_{IP}, amplitude of the I to P phase of the OJIP fluorescence transient (associated with PSI reaction center content). C (control); L1, L2, and L3 represent 100% garden soil, 90% garden soil + 10% Pb–Zn tailings, 75% garden soil + 25% Pb–Zn tailings, 50% garden soil + 50% Pb–Zn tailings, respectively. Different letters above the bars indicate a significant difference at $P < 0.05$. Values are means of $n = 6$, bar indicates standard error.

processes, such as stomatal opening, mesophyll conductance to CO_2, and the carboxylation capacity (Flexas et al., 2008; Centritto et al., 2009). In this study, although Gs and Gm significantly decreased (**Figures 2B, D**), they probably played a minor role in limiting photosynthesis because Ci and Cc increased simultaneously (**Table 3**, **Figures 2C, G**). The biochemical limitation was likely the major factor affecting photosynthesis in *M. azedarach* and *L. lucidum* (**Table 3**). Change for the results were in line with the findings of other studies (Seregin and Kozhevnikova, 2006; Velikova et al., 2011). The biochemical limitations were related to the considerable declines in V_{cmax} and J_{max} with increasing Pb–Zn stresses. The *M. azedarach* suffered more metabolic damage than that in *L. lucidum* (**Figures 2E, F**), indicating that the supply of energy source and carbon skeleton

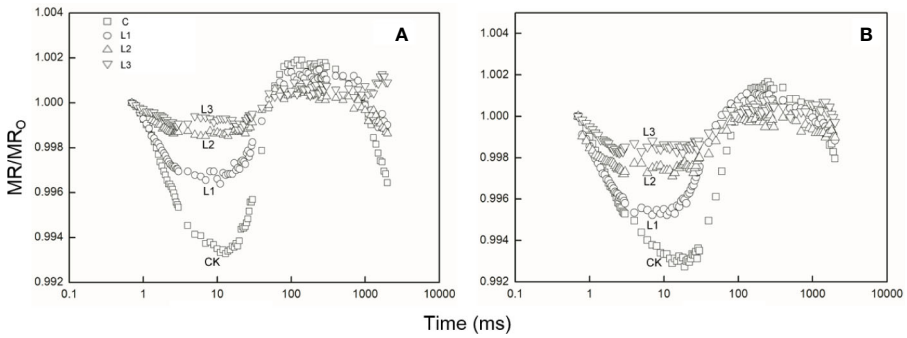

FIGURE 5 | The 820 nm light reflection curves of *M. azedarach* **(A)** and *L. lucidum* **(B)** in soil mixed with different proportions of Pb–Zn mine tailings. Modulated 820 nm reflection was expressed as MR/MR$_O$, where MR$_O$ is the modulated reflection value at the onset of actinic illumination (taken at 0.7 ms, the first reliable MR measurement) and MR is the modulated reflection signal during illumination. C (control); **(A)** L1, **(B)** L2, and **(C)** L3 represent 100% garden soil, 90% garden soil + 10% Pb–Zn tailings, 75% garden soil + 25% Pb–Zn tailings, 50% garden soil + 50% Pb–Zn tailings, respectively.

for plant growth and development was lower in *M. azedarach* than in *L. lucidum* (Imsande and Touraine, 1994). The decrease of V_{cmax} values might be ascribed to a reduction of Rubisco activity in the photosynthetic process (**Figure 2H**). The influence of Rubisco activity due to adverse environmental conditions has been reported by other studies (Bah et al., 2010). The J_{max} inhibition in the leaves under Pb–Zn tailing treatments observed from the changes in A/Cc curves indicated the photochemical limitation occurred in our study. The results were in line with the finding which Velikova et al. (2011) reported that alterations in the electron transport rate from PSII to PSI under heavy metals stresses result in a J_{max} limitation.

TABLE 4 | Parameters derived from the modulated 820-nm reflection (MR/MR$_O$) of the *M. azedarach* and *L. lucidum* grown in soil mixed with different proportions of Pb–Zn mining tailings.

M. azedarach	V_{PSI}	$V_{PSII-PSI}$	V_{PSII}
C	2.065 ± 0.212a	0.095 ± 0.008a	2.160 ± 0.145a
L1	1.309 ± 0.088b	0.063 ± 0.014b	1.372 ± 0.056b
L2	0.561 ± 0.107c	0.019 ± 0.007c	0.580 ± 0.009c
L3	0.413 ± 0.069d	0.005 ± 0.000d	0.418 ± 0.011d
L. lucidum			
C	2.046 ± 0.054a	0.036 ± 0.004a	2.082 ± 0.094a
L1	1.544 ± 0.131b	0.021 ± 0.006b	1.565 ± 0.083b
L2	1.804 ± 0.009c	0.010 ± 0.002c	1.814 ± 0.115c
L3	0.681 ± 0.102d	0.008 ± 0.001d	0.699 ± 0.057d

Data are means ± SE, n = 6. Different small letters in the same column indicate significant difference at 0.05 level by Duncan's new multiple test. V_{PSI}: maximum slope decrease of MR/MR$_O$; $V_{PSII-PSI}$: maximum slope increase of MR/MR$_O$; $V_{PSII} = V_{PSI} + V_{PSII-PSI}$. L1 90% garden soil + 10% Pb–Zn tailings, L2: 75% garden soil + 25% Pb–Zn tailings, L3: 50% garden soil + 50% Pb–Zn tailings.

In addition, there was a decrease in chlorophyll and carotenoid content with the rising Pb–Zn stress in *M. azedarach* and *L. lucidum*, which illustrated that Pb–Zn stress had harmed the photosynthetic apparatus for these two tree species. The decrease of chlorophyll content might be attributed to HMs interfering Fe metabolism, inhibiting chlorophyll synthetase activity and enhancing chlorophyll enzyme activity (Rana, 2015). As a result, chlorophyll degradation ultimately inactivated photosynthesis (Hajihashemi and Ehsanpour, 2013). We found that the decrease degree of chlorophyll content was higher than that of carotenoid content by HMs. The results were in line with the previous finding by Amir et al. (2020) who reported that chlorophylls were more susceptible to the negative impact of HMs as compared to carotenoids.

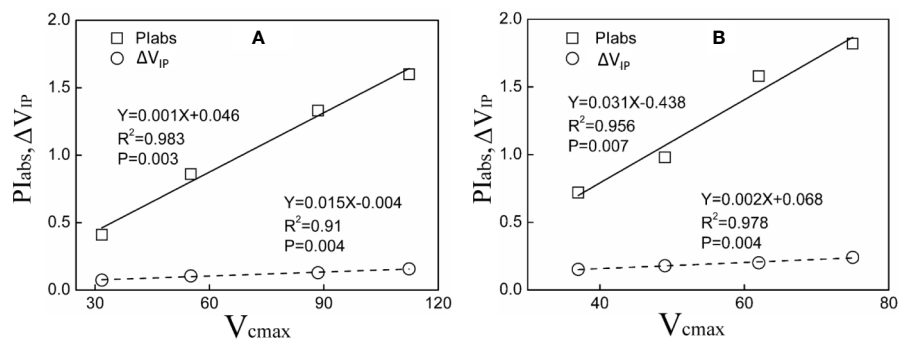

FIGURE 6 | Relationship between Plabs, ΔV_{IP} and V_{cmax} for *M. azedarach* **(A)** and *L. lucidum* **(B)** in soil mixed with different proportions of Pb–Zn mine tailings.

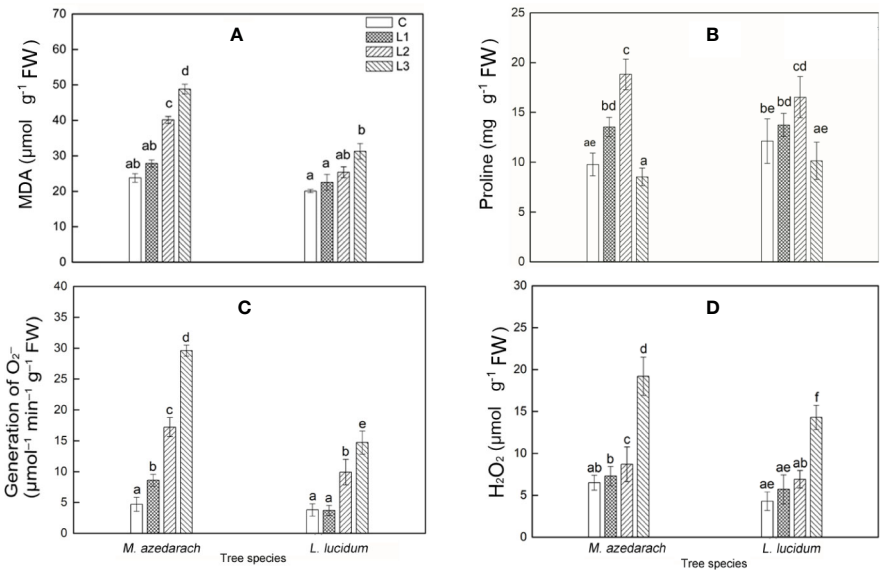

FIGURE 7 | Malondialdehyde (MDA) **(A)**, Proline **(B)**, O_2^- production rate **(C)**, H_2O_2 content **(D)** in leaves of *M. azedarach* and *L. lucidum* grown in soil mixed with different proportion of Pb–Zn mine tailings. C (control); L1, L2, and L3 represent 100% garden soil, 90% garden soil + 10% Pb–Zn tailings, 75% garden soil + 25% Pb–Zn tailings, 50% garden soil + 50% Pb–Zn tailings, respectively. Different letters above the bars indicate a significant difference at $P < 0.05$. Values are means of $n = 6$; bar indicates standard error.

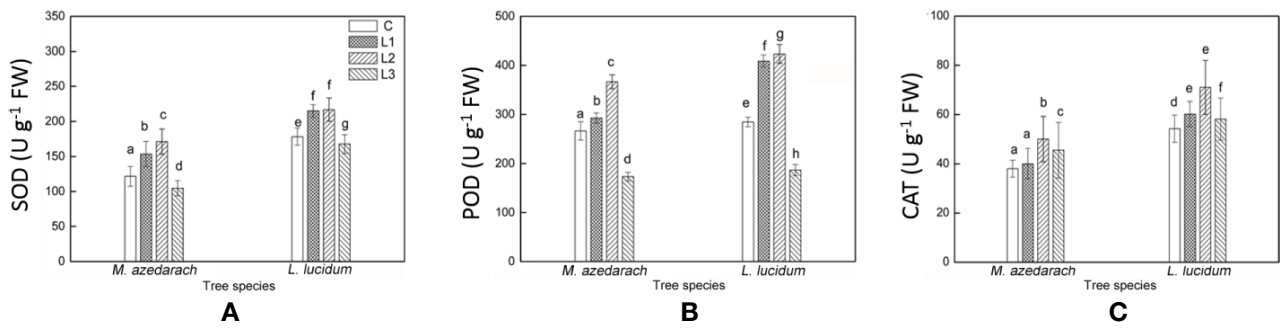

FIGURE 8 | Superoxide dismutase (SOD) **(A)**, Peroxidase (POD) **(B)** and Catalase (CAT) **(C)** in leaves of *M. azedarach* and *L. lucidum* grown in soil mixed with different proportions of Pb–Zn mine tailings. C (control); L1, L2, and L3 represent 100% garden soil, 90% garden soil + 10% Pb–Zn tailings, 75% garden soil + 25% Pb–Zn tailings, 50% garden soil + 50% Pb–Zn tailings, respectively. Different letters above the bars indicate a significant difference at $P < 0.05$. Values are means of $n = 6$; bar indicates standard error.

The Photosynthetic Electron Transport Is Altered by the Pb–Zn Tailing Stress

Changes in environmental factors could affect photosynthetic performance (Ji et al., 2018). The impacts of HM stresses on the electron transfer and energy balance in photosynthetic processes are quantified by OJIP fluorescence (Li and Zhang, 2015; Guo et al., 2018). In this study, the chlorophyll fluorescence transient curves of the two tested plants were all modified by Pb–Zn mine tailings (**Figure 3**). With the increase of proportions of Pb–Zn mine tailings, F_O values were significantly reduced in *M. azedarach*, but increased in *L. lucidum* compared to the control (**Figure 3**); the value of F_P decreased in the two tested plants. The F_O decrease in *M. azedarach* was likely attributed to the photoinhibitory damage on PSII acceptor (Setlik et al., 1990), and the increase of F_O in *L. lucidum* might be caused by increasing amount of free chlorophylls to the PSII RC (Gilmore et al., 1996). The decrease in F_P was observed in other heat and salt stress studies due to the increased fraction of inactive RCs (Jedmowski and Brüggemann, 2015; Oukarroum et al., 2015). W_K was the donor site parameter of PSII, which has been widely used to analyze damage to OEC by HM stresses (Li and Zhang, 2015). In this study, an increase of W_k value in *M. azedarach* (**Figure 4A**) suggested that Pb–Zn stress not only impaired the OEC; the process of electron transfer was also impaired at the P680 donor site (Jiang et al., 2008; Dąbrowski et al., 2016). However, the OEC and the donor side of PSII were

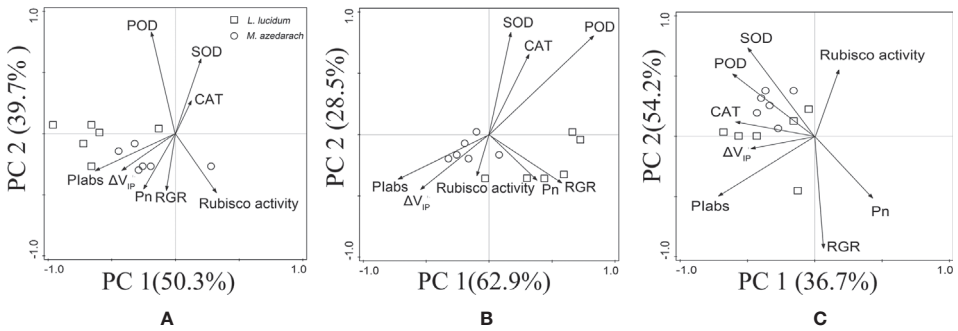

FIGURE 9 | Principal component analysis (PCA) of antioxidant enzymes, PSII performance, PSI content, net photosynthesis rates (Pn), and the relative growth rate (RGR) of *M. azedarach* and *L. lucidum* exposed to different proportions of Pb–Zn mine tailings. **(A)** L1, **(B)** L2, and **(C)** L3 represent 100% garden soil, 90% garden soil + 10% Pb–Zn tailings, 75% garden soil + 25% Pb–Zn tailings, 50% garden soil + 50% Pb–Zn tailings, respectively.

not impaired by Pb–Zn stress in *L. lucidum* since W_k values did not show a significant change.

Here, several important JIP-test parameters based on the OJIP transient were used to detect and quantify the changes of the photosystem status under Pb-Zn mine tailings stresses. The reduction of the maximum quantum yield of primary photochemistry (TRo/ABS) (**Figure 4D**) and the electron numbers moved further than the Q_A^- (ET_O/TR_O) (**Figure 4E**) indicating that Pb–Zn stress resulted in a fast accumulation of Q_A^- in the PSII reaction centers. The results suggested the photosynthetic electron transport was impaired in the acceptor side of PSII, and the electron flow beyond Q_A^- was blocked (Bernardini et al., 2016). It was reported that photoinhibition process can be more accurately assessed by the changes between flux ratios and specific fluxes per reaction center (RC) (Baker and Rosenqvist, 2004; Mlinarić et al., 2017). It was worth noting that the RC/CS_O was diminished and ABS/RC was risen in the two tested plants (**Figures 4C, F**), suggesting that although the numbers of active PSII RCs were decreased under Pb–Zn stress, the photochemical reaction efficiency of the remaining RCs was improved by maintaining the regular photosynthesis ability (Paunov et al., 2018). Due to the inactivation of a number of reaction centers, the remaining RCs had to increase their turnover in order to completely reduce the PQ pool (Zhou et al., 2019) as shown by a rise in parameter N (**Figure 4G**). *M. azedarach* had lower values of PIabs, RC/CS_O, TR_O/ABS, and ET_O/TR_O and higher values of ABS/RC than that in *L. lucidum*, indicating that Pb–Zn stress may affect, to a greater extent, the PSII activity in *M. azedarach* species.

ΔV_{IP} has been used to describe the changes in content of PSI reaction center under detrimental conditions (Oukarroum et al., 2009; Ceppi et al., 2012). The drought and Zn stress conditions declined ΔV_{IP} in *Hordeum spontaneum* (Oukarroum et al., 2009) and *Phragmites australis* (Bernardini et al., 2016). In this study, ΔV_{IP} was significantly lower for the two plants grown in Pb–Zn contaminated soil when compared to C (**Figure 4J**), indicating that Pb–Zn stress decreased the PSI reaction center in the two tested tree species. The significant reductions of φR_o and δR_o (**Figures 4H, I**) indicated that the effect of Pb–Zn stress on electron flow occurred in the acceptor side of PSI because of the reduction of the PSI content (Hu et al., 2018). In addition, the values of V_{PSI} of the two tested plants decreased in the Pb–Zn treated groups when compared to the C (**Figure 5**, **Table 4**), indicating that the oxidization reactions were inhibited due to the Pb–Zn stress. The decline in the $V_{PSII-PSI}$ suggested that the reduction activity of PSI activity was injured by the Pb–Zn stress. Therefore, the decreases in maximum oxidization and reduction activity of PSI reaction center were observed since Pb–Zn stress affected PSI content.

In this study, a positive linear relation was found between PI_{abs} and V_{cmax} in this study suggesting that PSII performance was positively related to CO_2 assimilation (**Figure 6**). The result was in accordance with the suggestions provided by Ghotbi-Ravandi et al. (2014); they reported that the reduction in PSII performance played an important role in the decrease of CO_2 assimilation rate in *Morocco* under mild and severe drought stresses. Meanwhile, ΔV_{IP} also decreased linearly with the decrease of V_{cmax}; the result suggested that PSI content might limit the capacity of CO_2 assimilation (**Figure 6**). Because the decrease of PSI content could disturb the electron flow from PSII to PSI and limited the synthesis of ATP and NADPH (Brestic et al., 2015), the inhibition of CO_2 assimilation rate can be suggested as a result of the excessive excitation energy that damage the photosystems and especially impeded the photochemical activity of PSI (Zivcak et al., 2013). Specifically, *M. azedarach* suffered more serious effects on the photosynthetic electron transport chain than *L. lucidum* under Pb–Zn stress. This finding was supported by the fact that photosynthetic parameters (PIabs, ΔV_{IP}, and Pn) were more affected in *M. azedarach* than that in *L. lucidum* in PCA analysis (**Figure 9**).

L. lucidum May Be More Tolerant to Pb–Zn Stress Than *M. azedarach*

It is previously demonstrated that adverse conditions impaired PSII electron transport; the excess electron resulted in increasing the levels of ROS and consequently caused oxidative stress (Pospíšil, 2009; Guo et al., 2018). The malondialdehyde (MDA) content represents level of lipid peroxidation, which was able to indicate

oxidative damage of membrane lipids under stress conditions (Sharma and Dubey, 2005). In this study, with the increase of proportion of Pb–Zn mine tailings, the O_2^- production rate and H_2O_2 content in both tested tree leaves increased significantly, contributing to a significant increase of MDA content. This result was in line with the previous reports where MDA content increased in *Peganum harmala*, *Kandelia obovate*, and *Alternanthera bettzickiana* under HMs stress (Lu et al., 2010; Cheng et al., 2017). In this study, proline contents increased in *M. azedarach* and *L. lucidum* leaves in L1 and L2 treatments but decreased at L3 treatments when compared to the C (**Figure 7B**). The phenomena suggested the increase of proline contents at low and medium Pb–Zn treatments could maintain the integrity of cellular membranes, protect proton pump, and eliminate ROS (Dhir et al., 2012). The decrease of proline contents in L3 treatments might be explained by the fact that the physiological functions and metabolisms of plants were seriously damaged at high concentration of Pb–Zn toxicity (Chen et al., 2003). When the equilibrium between ROS generation and detoxification was disrupted by abiotic stresses, the induction of antioxidative enzyme defense activities played a crucial role in HM tolerance in plants (Ashraf, 2009). SOD was the first defense line against oxidative stresses, and superoxide radicals (O_2^-) were scavenged by SOD. CAT was recognized as the most important enzyme for scavenging H_2O_2 produced in plant cells and was primarily associated with the maintenance steady of cellular. POD enzyme can detoxify H_2O_2 and thereby was conducive to maintaining the integrity of cellular membranes (Liu et al., 2017). In this study, SOD, POD, and CAT activity in *M. azedarach* and *L. lucidum* initially increased and then declined under Pb–Zn stress (**Figure 8**). The same patterns were found in *Iris halophila* exposed to Pb mine tailing treatments (Han et al., 2016). The SOD, POD, and CAT activities were higher in the L1 and L2 treatments than those in the C, indicating that the antioxidative system can effectively mitigate oxidative damage (Nie et al., 2016). The reduction of antioxidative enzyme activity under the highest Pb–Zn tailing treatments might be ascribed to the fact that the gene expression of SOD, POD and CAT enzymes was impacted by strong Pb–Zn stress (Hu et al., 2015). Another account for the decrease in SOD, POD, and CAT activity was that these variables were exhausted to alleviate the detrimental effects of ROS under higher Pb–Zn stress (Nie et al., 2016).

Under Pb–Zn stress, *L. lucidum* had a lower level of lipid peroxidation and higher activities of the antioxidative enzyme when compared to *M. azedarach*. As the tolerance to HMs was linked with the low level of lipid peroxidation and high activities of antioxidative enzymes (Ma et al., 2001; Sharma and Dietz, 2009), *L. lucidum* likely possessed a higher tolerability to HMs than *M. azedarach*. Additionally, less influence occurred on PSII and PSI in *L. lucidum* than in *M. azedarach* (**Figure 4**), which was probably attributed to the lower MDA content and higher antioxidative enzyme activities in *L. lucidum* (Iqbal et al., 2019). It should be noted that the TFs for Pb and Zn in stems and leaves were lower in *L. lucidum* than in *M. azedarach*, and more Pb and Zn were retained in *L. lucidum* roots, indicating that *L. lucidum* has more excellent metal exclusion strategy under Pb–Zn mine tailing treatments.

CONCLUSION

The current study showed that Pb–Zn mine tailing had a crucial negative influence on two tested plants' development and biomass production by inhibiting the chlorophyll synthesis and photosynthetic metabolism. The reduction of net photosynthetic rates in *M. azedarach* and *L. lucidum* due to HM stress was mainly caused by their biochemical limitation, including decreases of V_{cmax} and J_{max}. Pb–Zn stress damaged multiple locations along the photosynthetic electron transport chain. Specifically, it impaired the OEC (only in *M. azedarach*) and blocked electron flow of acceptor side of PSII and disturbed the PSI oxidation and reduction in both tested trees. Moreover, the increase of ROS content in both plant species was directly related to the obstruction of the electron transfer. Meanwhile, *M. azedarach* and *L. lucidum* could maintain high levels of SOD, POD, CAT, and proline contents to effectively relieve oxidative stress. The more tolerance of *L. lucidum* might be attributed to these facts: (1) higher RGR; (2) more accumulation of Pb–Zn in roots; (3) a less extent effect occurred on PSII and PSI activity; and (4) lower ROS and MDA content and higher antioxidative enzymes activities.

DATA AVAILABILITY STATEMENT

All datasets presented in this study are included in the article.

AUTHOR CONTRIBUTIONS

Idea and study designed: FZ. Performed the experiments: ML and HX. Wrote the paper: XH. Helped revise original paper: XC, ZH, and GW.

FUNDING

This work was financially supported by the Key Research and Development Project of Hunan Province (2017NK2171), the "948" introduction project of The State Bureaucracy of Forestry (2014-4-62), the Hunan Provincial Innovation Foundation For Postgraduate (CX2018B434), the Scientific Innovation Fund for Post-graduates of Central South University of Forestry and Technology (20181007), and the Scientific Innovation Fund for Post-graduates of Central South University of Forestry and Technology (CX20192062).

ACKNOWLEDGMENTS

We thank Dr. DaYong Fan for stimulating discussions and critical readings of the manuscript.

REFERENCES

Aebi, H. (1984). Catalase in vitro. *Methods Enzymol.* 105, 121–126. doi: 10.1016/S0076-6879(84)05016-3

Amir, W., Farid, M., Ishaq, H. K., Farid, S., Zubair, M., Alharby, H. F., et al. (2020). Accumulation potential and tolerance response of Typha latifolia L. under citric acid assisted phytoextraction of lead and mercury. *Chemosphere* 157, 127247–127261. doi: 10.1016/j.chemosphere.2020.127247

Ashraf, M. (2009). Biotechnological approach of improving plant salt tolerance using antioxidants as markers. *Biotechnol. Adv.* 1, 84–93. doi: 10.1016/j.biotechadv.2008.09.003

Bah, A. M., Sun, H., Chen, F., Zhou, J., Dai, H. X., Zhang, G. P., et al. (2010). Comparative proteomic analysis of typha angustifolia leaf under chromium, cadmium and lead stress. *J. Hazard. Mater.* 184, 191–203. doi: 10.1016/j.jhazmat.2010.08.023

Baker, N. R., and Rosenqvist, E. (2004). Applications of chlorophyll fluorescence can improve crop production strategies: An examination of future possibilities. *J. Exp. Bot.* 55, 1607–1621. doi: 10.1093/jxb/erh196

Bao, S. D. (2000). *The Soil Agricultural Chemistry Analysis* (Beijing: Chinese Agriculture Press). (in chinese).

Beffa, R., Martin, H. V., and Pilet, P. E. (1990). In vitro oxidation of indoleacetic acid by soluble auxin-oxidases and peroxidases from maize root. *Plant Physiol.* 94, 485–491. doi: 10.1104/pp.94.2.485

Belatik, A., Hotchandani, S., Tajmir-Riahi, H.-A., and Carpentier, R. (2013). Alteration of the structure and function of photosystem I by Pb^{2+}. *J. Photochem. Photobiol. B.* 123, 41–47. doi: 10.1016/j.jphotobiol.2013.03.010

Bernacchi, C. J., Portis, A. R., Nakano, H., Caemmerer, S. V., and Long, S. P. (2002). Temperature response of mesophyll conductance. Implications for the determination of Rubisco enzyme kinetics and for limitations to photosynthesis in vivo. *Plant Physiol.* 130, 1992–1998. doi: 10.1104/pp.008250

Bernardini, A., Salvatori, E., Guerrini, V., Fusaro, L., Canepari, S., and Manes, F. (2016). Effects of high Zn and Pb concentrations on Phragmites australis (Cav.) Trin. Ex. Steudel: Photosynthetic performance and metal accumulation capacity under controlled conditions. *Int. J. Phytoremediat.* 1, 16–24. doi: 10.1080/15226514.2015.1058327

Bezerril, F. N. M., Otoch, M. D. L. O., Gomes-Rochette, N. F., Sobreira, A.C.de M., Barreto, A. A. G. C., de Oliveira, F. D. B., et al. (2017). Effect of lead on physiological and antioxidant responses in two Vigna unguiculata cultivars differing in Pb-accumulation. *Chemosphere* 176, 397–404. doi: 10.1016/j.chemosphere.2017.02.072

Bi, A., Fan, J., Hu, Z., Wang, G., Amombo, E., Fu, J., et al. (2016). Differential acclimation of enzymatic antioxidant metabolismand photosystem II photochemistry in Tall Fescue under drought and heat and the combined stresses. *Front. Plant Sci.* 7, 453. doi: 10.3389/fpls.2016.00453

Boominathan, R., and Doran, P. M. (2003). Cadmium tolerance and antioxidative defenses in hairy roots of the cadmium hyperaccumulator, Thlaspi caerulescens. *Biotechnol. Bioeng.* 83, 158–167. doi: 10.1002/bit.10656

Brestic, M., Zivcak, M., Kunderlikova, K., Sytar, O., Shao, H., Kalaji, H. M., et al. (2015). Low PSI content limits the photoprotection of PSI and PSII in early growth stages of chlorophyll b-deficient wheat mutant lines. *Photosynth. Res.* 125, 151–166. doi: 10.1007/s11120-015-0093-1

Centritto, M., Loreto, F., and Chartzoulakis, K. (2003). The use of low [CO_2] to estimate diffusional and non-diffusional limitations of photosynthetic capacity of salt-stressed olive saplings. *Plant Cell Environ.* 26, 585–594. doi: 10.1046/j.1365-3040.2003.00993.x

Centritto, M., Lauteri, M., Monteverdi, M. C., and Serraj, R. (2009). Leaf gas exchange, carbon isotope discrimination, and grain yield in contrasting rice genotypes subjected to water deficits during the reproductive stage. *J. Exp. Bot.* 60, 2325–2339. doi: 10.1093/jxb/erp123

Ceppi, M. G., Oukarroum, A., Çiçek, N., Strasser, R. J., and Schansker, G. (2012). The IP amplitude of the fluorescence rise OJIP is sensitive to changes in the photosystem I content of leaves: a study on plants exposed to magnesium and sulfate deficiencies, drought stress and salt stress. *Physiol. Plant* 144, 277–288. doi: 10.1111/j.1399-3054.2011.01549.x

Chen, Y. X., He, Y. F., Luo, Y. M., Yu, Y. L., Lin, Q., and Wong, M. H. (2003). Physiological mechanism of plant roots exposed to cadmium. *Chemosphere* 6, 780–793. doi: 10.1016/s0045-6535(02)00220-5

Chen, L. S., Qi, Y. P., Smith, B. R., and Liu, X. H. (2005). Aluminum-induced decrease in CO_2 assimilation in citrus seedlings is unaccompanied by decreased activities of key enzymes involved in CO_2 assimilation. *Tree Physiol.* 25, 317–324. doi: 10.1093/treephys/25.3.317

Chen, F. L., Wang, S. Z., Mu, S. Y., Azimuddin, I., Zhang, D. Y., Pan, X. L., et al. (2015). Physiological responses and accumulation of heavy metals and arsenic of Medicago sativa L. growing on acidic copper mine tailings in arid lands. *J. Geochem. Explor.* 157, 27–35. doi: 10.1016/j.gexplo.2015.05.011

Cheng, S. S., Tam, N. F. Y., Li, R. L., Shen, X. X., Niu, Z. Y., Chai, M. W., et al. (2017). Temporal variations in physiological responses of Kandelia obovata seedlings exposed to multiple heavy metals. *Mar. Pollut. Bull.* 2, 1089–1095. doi: 10.1016/j.marpolbul.2017.03.060

Chiang, H. C., Lo, J. C., and Yeh, K. C. (2006). Genes Associated with Heavy MetalTolerance and Accumulation in Zn/Cd Hyperaccumulator Arabidopsis halleri: A GenomicSurvey with cDNA Microarray. *Environ. Sci. Technol.* 40, 6792–6798. doi: 10.1021/es061432y

Chu, J. J., Zhu, F., Chen, X. Y., Liang, H. Z., Wang, R. J., Wang, X. X., et al. (2018). Effects of cadmium on photosynthesis of Schima superba young plant detected by chlorophyll fluorescence. *Environ. Sci. Pollut. R.* 25, 10679–10687. doi: 10.1007/s11356-018-1294-x

Çiçek, N., Oukarroum, A., Strasser, R. J., and Schansker, G. (2017). Salt stress effects on the photosynthetic electron transport chain in two chickpea lines differing in their salt stress tolerance. *Photosynth. Res.* 136, 291–301. doi: 10.1007/s11120-017-0463-y

Dąbrowski, P., Baczewska, A. H., and Pawluśkiewicz, B. (2016). Prompt chlorophyll a fluorescence as a rapid tool for diagnostic changes in PSII structure inhibited by salt stress in Perennial ryegrass. *J. Photochem. Photobiol. B.* 157, 22–31. doi: 10.1016/j.jphotobiol.2016.02.001

Deng, G., Li, M., Li, H., Yin, L., and Li, W. (2014). Exposure to cadmium causes declines in growth and photosynthesisin the endangered aquatic fern (*Ceratopteris pteridoides*). *Aquat. Bot.* 1, 23–32. doi: 10.1016/j.aquabot.2013.07.003

Dhindsa, R. S., Plumb-Dhindsa, P., and Thorpe, T. A. (1981). Leaf senescence: correlated with increased levels of membrane permeability and lipid peroxidation, and decreased levels of superoxide dismutase and catalase. *J. Exp. Bot.* 32, 93–101. doi: 10.1093/jxb/32.1.93

Dhir, B., Nasim, S. A., Samantary, S., and Srivastava, S. (2012). Assessment of osmolyte accumulation in heavy metal exposed *Salvinia Natans*. *Int. J. Bot.* 8, 153–158. doi: 10.3923/ijb.2012.153.158

Du, H. M., Huang, Y., Qu, M., Li, Y. H., Hu, X. Q., Yang, W., et al. (2020). A Maize ZmAT6 gene confers Aluminum tolerance via reactive oxygen species scavenging. *Front. Plant Sci.* 11, 1016. doi: 10.3389/fpls.2020.01016

Farquhar, G. D., Caemmerer, S. V., and Berry, J. A. (1980). A biochemical model of photosynthetic CO_2 assimilation in leaves of C3 species. *Planta* 149, 78–90. doi: 10.1007/BF00386

Flexas, J., Ribas-Carbò, M., Diaz-Espejo, A., Galmés, J., and Medrano, H. (2008). Mesophyll conductance to CO_2: current knowledge and future prospects. *Plant Cell Environ.* 31, 602–621. doi: 10.1111/j.1365-3040.2007.01757.x

Frérot, H., Lefèbvre, C., Gruber, W., Collin, C., Santos, A. D., and Escarré, J. (2006). Specific Interactions between Local Metallicolous Plants Improve the Phytostabilization of Mine Soils. *Plant Soil.* 282, 53–65. doi: 10.1007/s11104-005-5315-4

Gao, J., Li, P., Ma, F., and Goltsev, V. (2014). Photosynthetic performance during leaf expansion in Malus micromalus probed by chlorophyll a fluorescence and modulated 820 nm reflection. *J. Photochem. Photobiol. B.* 137, 144–150. doi: 10.1016/j.jphotobiol.2013.12.005

Gao, J. F. (2006). *Experimental Guidance For Plant Physiology* (Beijing, China (in chinese: Higher Education Press). doi: 10.4236/oalib.preprints.1200091

Ghotbi-Ravandi, A. A., Shahbazi, M., Shariati, M., and Mulo, P. (2014). Effects of Mild and Severe Drought Stress on Photosynthetic Efficiency in Tolerant and Susceptible Barley (*Hordeum vulgare* L.) Genotypes. *J. Agron. Crop Sci.* 26, 403–415. doi: 10.1111/jac.12062

Giannopolitis, C. N., and Ries, S. K. (1977). Superoxide dismutases I. Occurrence in higher plants. *Plant Physiol.* 59, 309–314. doi: 10.1104/pp.59.2.309

Gilmore, A. M., Hazlett, T. L., and Debrunner, P. G. (1996). Comparativetime-resolved photosystem II chlorophyll a fluorescence analyses revealdistinctive differences between photoinhibitory reaction center damage andxanthophyll cycle-dependent energy dissipation. *Photochem. Photobiol.* 64, 552–563. doi: 10.1111/j.1751-1097.1996.tb03105.x

Grassi, G., and Magnani, F. (2005). Stomatal, mesophyll conductance and biochemical limitations to photosynthesis as affected by drought and leaf

ontogeny in ash and oak trees. *Plant Cell Environ.* 28, 834–849. doi: 10.1111/j.1365-3040.2005.01333.x

Guo, P., Qi, Y. P., Cai, Y. T., Yang, T. Y., Yang, L. T., Huang, Z. R., et al. (2018). Aluminum effects on photosynthesis, reactive oxygen species and methylglyoxal detoxification in two *citrus* species differing in aluminum tolerance. *Tree Physiol.* 38, 1548–1565. doi: 10.1093/treephys/tpy035

Ha, N. T. H., Sakakibara, M., Sano, S., and Nhuan, M. T. (2011). Uptake of metals and metalloids by plants growing in a lead–zinc mine area, northern vietnam. *J. Hazard. Mater.* 186, 1384–1391. doi: 10.1016/j.jhazmat.2010.12.020

Hajihashemi, S., and Ehsanpour, A. A. (2013). Influence of exogenously applied paclobutrazol on some physiological traits and growth of Stevia rebaudiana under in vitro drought stress. *Biologia* 68, 414–420. doi: 10.2478/s11756-013-0165-7

Han, Y. L., Huang, S. Z., Yuan, H. Y., Zhao, J. Z., and Gu, J. G. (2013). Organic acids on the growth, anatomical structure, biochemical parameters and heavy metal accumulation of Iris lactea var. chinensis seedling growing in Pb mine tailings. *Ecotoxicology* 22, 1033–1042. doi: 10.1007/s10646-013-1089-2

Han, Y. L., Zhang, L. L., Yang, Y. H., Yuan, H. Y., Zhao, J. Z., Gu, J. G., et al. (2016). Pb uptake and toxicity to Iris halophila tested on Pb mine tailing materials. *Environ. Pollut.* 214, 510–516. doi: 10.1016/j.envpol.2016.04.048

Harley, P. C., Loreto, F., Dimarco, G., and Sharkey, T. D. (1992). Theoretical considerations when estimating the mesophyll conductance to CO_2 flux by analysis of the response of photosynthesis to CO_2. *Plant Physiol.* 98, 1429–1436. doi: 10.1104/pp.98.4.1429

Hu, Z. R., Fan, J. B., Chen, K., Amombo, E., Chen, L., and Fu, J. M. (2015). Effects of ethylene on photosystem II and antioxidant enzyme activity in Bermuda grass under low temperature. *Photosynth. Res.* 128, 59–72. doi: 10.1007/s11120-015-0199-5

Hu, W., Snider, J. L., Chastain, D. R., Slaton, W., and Tishchenko, V. (2018). Sub-optimal emergence temperature alters thermotolerance of thylakoid component processes in cotton seedlings. *Environ. Exp. Bot.* 155, 360–367. doi: 10.1016/j.envexpbot.2018.07.020

Huang, X. H., Zhu, F., Yan, W. D., Chen, X. Y., Wang, G. J., and Wang, R. J. (2019). Effects of Pb and Zn toxicity on chlorophyll fluorescence and biomass production of *Koelreuteria paniculata* and *Zelkova schneideriana* young plants. *Photosynthetica* 52, 688–697. doi: 10.32615/ps.2019.050

Imsande, J., and Touraine, B. (1994). Demand and the regulation of nitrate uptake. *Plant Physiol.* 105, 3–7. doi: 10.1104/pp.105.1.3

Iqbal, N., Hussain, S., Raza, M. A., Yang, C. Q., Safdar, M. E., Brestic, M., et al. (2019). Drought tolerance of soybean (*Glycine max L. Merr.*) by improved photosynthetic characteristics and an efficient antioxidant enzyme activities under a split-root system. *Front. Physiol.* 10, 786. doi: 10.3389/fphys.2019.00786

Israr, M., Jewell, A., Kumar, D., and Sahi, S. V. (2011). Interactive effects of lead, copper, nickel and zinc on growth, metal uptake and antioxidative metabolism of Sesbania drummondii. *J. Hazard. Mater.* 186, 1520–1526. doi: 10.1016/j.jhazmat.2010.12.021

Jedmowski, C., and Brüggemann, W. (2015). Imaging of fast chlorophyll fluorescence induction curve (OJIP) parameters, applied in a screening study with wild barley (*Hordeum spontaneum*) genotypes under heat stress. *J. Photoch. Photobio. B.* 151, 153–160. doi: 10.1016/j.jphotobiol.2015.07.020

Ji, X., Cheng, J., Gong, D. H., Zhao, X. J., Qi, Y., Su, Y. N., et al. (2018). The effect of NaCl stress on photosynthetic efficiency and lipid production in freshwater microalg—*scenedesmus obliquus*, xj002. *Sci. Total Environ.* 633, 593–599. doi: 10.1016/j.scitotenv.2018.03.240

Jiang, H., Chen, L., Zheng, J. G., Han, S., Tang, N., and Smith, B. R. (2008). Aluminum-induced effects on photosystem II photochemistry in citrus leaves assessed by the chlorophyll a fluorescence transient. *Tree Physiol.* 28, 1863–1871. doi: 10.1093/treephys/28.12.1863

Kola, H., and Wilkinson, K. J. (2005). Cadmium uptake by a green alga can be predicted by equilibrium modelling. *Environ. Sci. Technol.* 9, 3040–3047. doi: 10.1021/es048655d

Kosobrukhov, A., Knyazeva, I., and Mudrik, V. (2004). Plantago major plants responses to increase content of lead in soil: growth and photosynthesis. *Plant Growth Regul.* 2, 145–151. doi: 10.1023/b:grow.0000017490.59607.6b

Krantev, A., Yordanova, R., Janda, T., Szalai, G., and Popova, L. (2008). Treatment with salicylic acid decreases the effect of cadmium on photosynthesis in maize plants. *J. Plant Physiol.* 9, 920–931. doi: 10.1016/j.jplph.2006.11.014

Laisk, A., and Loreto, F. (1996). Determining photosynthetic parameters from leaf CO_2 exchange and chlorophyll fluorescence–Ribulose-1,5-bisphosphate carboxylase oxygenase specificity factor, dark respiration in the light, excitation distribution between photosystems, alternative electron transport and mesophyll diffusion resistance. *Plant Physiol.* 110, 903–912. doi: 10.1104/pp.110.3.903

Li, X. M., and Zhang, L. H. (2015). Endophytic infection alleviates Pb^{2+} stress effects on photosystem II functioning of *Oryza sativa* leaves. *J. Hazard. Mater* 295, 79–85. doi: 10.1016/j.jhazmat.2015.04.015

Li, M. S. (2006). Ecological restoration of mineland with particular reference to the metalliferous mine wasteland in China: a review of research and practice. *Sci. Total Environ.* 357, 38–53. doi: 10.1016/j.scitotenv.2005.05.003

Liang, H. Z., Zhu, F., Wang, R. J., Huang, X. H., and Chu, J. J. (2019). Photosystem II of Ligustrum lucidumin response to different levels of manganese exposure. *Sci. Rep.* 9, 12568–12578. doi: 10.1038/s41598-019-48735-8

Lin, M. Z., and Jin, M. F. (2018). Soil Cu contamination destroys the photosynthetic systems and hampers the growth of green vegetables. *Photosynthetica* 56, 1336–1345. doi: 10.1007/s11099-018-0831-7

Liu, H., Zhang, C., Wang, J., Zhou, C., Feng, H., Mahajan, M. D., et al. (2017). Influence and interaction of iron and cadmium on photosynthesis and antioxidative enzymes in two rice cultivars. *Chemosphere* 171, 240–247. doi: 10.1016/j.chemosphere.2016.12.081

Lu, Y., Li, X. R., He, M. Z., Zhao, X., Liu, Y. B., Cui, Y., et al. (2010). Seedlings growth and antioxidative enzymes activities in leaves under heavy metal stress differ between two desert plants: a perennial (Peganum harmala) and an annual (*Halogeton glomeratus*) grass. *Acta Physiol. Plant* 3, 583–590. doi: 10.1007/s11738-009-0436-7

Lu, T., Meng, Z., Zhang, G., Qi, M., Sun, Z., Liu, Y., et al. (2017). Sub-high Temperature and High Light Intensity Induced Irreversible Inhibition on Photosynthesis System of Tomato Plant (*Solanum lycopersicum* L.). *Front. Plant Sci.* 8, 365. doi: 10.3389/fpls.2017.00365

Luo, Z. H., Tian, D. L., Ning, C., Yan, W. D., Xiang, W. H., and Peng, C. H. (2015). Roles of *Koelreuteria bipinnata* as a suitable accumulator tree species in remediating Mn, Zn, Pb, and Cd pollution on Mn mining wastelands in southern China. *Environ. Earth Sci.* 74, 4549–4559. doi: 10.1007/s12665-015-4510-8

Ma, L. Q., Komar, K. M., Tu, C., Zhang, W., Cai, Y., and Kennelley, E. D. (2001). A fern that hyperaccumulates arsenic: a hardy, versatile, fast growing plant helps to remove arsenic from contaminated soils. *Nature* 6820, 579. doi: 10.1038/35054664

Mallick, N., and Mohn, F. H. (2003). Use of chlorophyll fluorescence in metalstress research: a case study with the green microalga Scenedesmus. *Ecotoxicol. Environ. Saf.* 55, 64–69. doi: 10.1016/s0147-6513(02)00122-7

Meeinkuirt, W., Pokethitiyook, P., Kruatrachue, M., Tanhan, P., and Chaiyarat, R. (2012). Phytostabilization of a pb-contaminated mine tailing by various tree species in pot and field trial experiments. *Int. J. Phytoremediat.* 14, 925–938. doi: 10.1080/15226514.2011.636403

Mlinarić, S., Antunović Duni, J., Skendrović Babojelić, M., Cesar, V., and Lepeduš, H. (2017). Differential accumulation of photosynthetic proteins regulates diurnal photochemical adjustments of PSII in common fig (*Ficus carica* L.) leaves. *J. Plant Physiol.* 209, 1–10. doi: 10.1016/j.jplph.2016.12.002

Mobin, M., and Khan, N. A. (2007). Photosynthetic activity, pigment composition and antioxidative response of two mustard (*Brassica juncea*) cultivars differing in photosynthetic capacity subjected to cadmium stress. *J. Plant Physiol.* 164, 601–610. doi: 10.1016/j.jplph.2006.03.003

Nie, J., Liu, Y. G., Zeng, G. M., Zheng, B. H., Tan, X. F., Liu, H., et al. (2016). Cadmium accumulation and tolerance of macleaya cordata: a newly potential plant for sustainable phytoremediation in cd-contaminated soil. *Environ. Sci. Pollut. R.* 23, 10189–10199. doi: 10.1007/s11356-016-6263-7

Okuda, T., Matsuda, Y., Yamanaka, A., and Sagisaka, S. (1991). Abrupt increase in the level of hydrogen peroxide in leaves of winter wheat is caused by cold treatment. *Plant Physiol.* 97, 1265–1267. doi: 10.1104/pp.97.3.1265

Oukarroum, A., Schansker, G., and Strasser, R. J. (2009). Drought stress effects on photosystem I content and photosystem II thermotolerance analyzed using Chl a fluorescence kinetics in barley varieties differing in their drought tolerance. *Physiol. Plant* 137, 188–199. doi: 10.1111/j.1399-3054.2009.01273.x

Oukarroum, A., Bussotti, F., Goltsev, V., and Kalaji, H. M. (2015). Correlation between reactive oxygen species production and photochemistry of

photosystems I and II in Lemna gibba l plants under salt stress. *Environ. Exp. Bot.* 109, 80–88. doi: 10.1016/j.envexpbot.2014.08.005

Paunov, M., Koleva, L., Vassilev, A., Vangronsveld, J., and Goltsev, V. (2018). Effects of different metals on photosynthesis: cadmium and zinc affect chlorophyll fluorescence in Durum Wheat. *Int. J. Mol. Sci.* 19, 787–800. doi: 10.3390/ijms19030787

Pierattini, E. C., Francini, A., Raffaelli, A., and Sebastiani, L. (2017). Surfactant and heavy metal interaction in poplar: a focus on SDS and Zn uptake. *Tree Physiol.* 38, 109–118. doi: 10.1093/treephys/tpx155

Pinelli, P., and Loreto, F. (2003). $^{12}CO_2$ emission from different metabolic pathways measured in illuminated and darkened C3 and C4 leaves at low, atmospheric and elevated CO_2 concentration. *J. Exp. Bot.* 54, 1761–1769. doi: 10.1093/jxb/erg187

Pospíšil, P. (2009). Production of reactive oxygen species by photosystem II. *Biochim. Biophys. Acta* 1787, 1151–1160. doi: 10.1016/j.bbabio.2009.05.005

Pulford, I. D., and Watson, C. (2003). Phytoremediation of heavy metal-contaminated land by trees—a review. *Environ. Int.* 29, 529–540. doi: 10.1016/s0160-4120(02)00152-6

Rana, S. (2015). Plant response towards cadmium toxicity: an overview. *Ann. Plant Sci.* 7, 1162–1172.

Sagardoy, R., Vázquez, S., Florez-Sarasa, I. D., Albacete, A., Ribas-Carbó, M., Flexas, J., et al. (2010). Stomatal and mesophyll conductances to CO_2 are the main limitations to photosynthesis in sugar beet (beta vulgaris) plants grown with excess zinc. *New Phytol.* 187, 145–158. doi: 10.1111/j.1469-8137.2010.03241.x

Seregin, I. V., and Kozhevnikova, A. D. (2006). Physiological role of nickel and its toxic effects on higher plants. *Russ. J. Plant Physiol.* 53, 257–277. doi: 10.1134/s1021443706020178

Setlik, I., Allakhveridiev, S.II, Nedbal, L., Setlikova, E., and Klimov, V. V. (1990). Three types of Photosystem II photoinactivation-I. Damaging process on the acceptor side. *Photosynth. Res.* 23, 39–48. doi: 10.1007/BF00030061

Sharkey, T. D., Bernacchi, C. J., Farquha, G. D., and Singsaas, E. L. (2007). Fitting photosynthetic carbon dioxide response curves for C3 leaves. *Plant Cell Environ.* 30, 1035–1040. doi: 10.1111/j.1365-3040.2007.01710.x

Sharma, S. S., and Dietz, K. J. (2009). The relationship between metal toxicity and cellular redox imbalance. *Trends Plant Sci.* 1, 0–50. doi: 10.1016/j.tplants.2008.10.007

Sharma, P., and Dubey, R. S. (2005). Lead toxicity in plants. *Toxic Met. Plants* 17, 35–52. doi: 10.1515/9783110434330-015

Sigfridsson, K. G., Bernat, G., Mamedov, F., and Styring, S. (2004). Molecular interference of Cd^{2+} with photosystem II. *BBA-Biomembranes* 1659, 19–31. doi: 10.1016/j.bbabio.2004.07.003

Sorrentino, M. C., Capozzi, F., Amitrano, C., Giordano, S., Arena, C., and Spagnuolo, V. (2018). Performance of three cardoon cultivars in an industrial heavy metal-contaminated soil: Effects on morphology, cytology and photosynthesis. *J. Hazard. Mater* 351, 131–137. doi: 10.1016/j.jhazmat.2018.02.044

Srivastava, M., and Doran, P. M. (2005). Antioxidant responses of hyperaccumulator and sensitive fern species to arsenic. *J. Exp. Bot.* 56, 1335–1342. doi: 10.1093/jxb/eri134

Štefanić, P. P., Cvjetko, P., Biba, R., Domijan, A. M., Letofsky-Papst, I., Tkalec, M., et al. (2018). Physiological, ultrastructural and proteomic responses of tobacco seedlings exposed to silver nanoparticles and silver nitrate. *Chemosphere* 209, 640–653. doi: 10.1016/j.chemosphere.2018.06.128

Strasser, R. J., Tsimilli-Michael, M., and Srivastava, A. (2004). "Analysis of the chlorophyll a fluorescence transient," in *Chlorophyll fluorescence: a signature of photosynthesis*. Eds. G. C. Papageorgiou and Govindjee, (Netherlands: Kluwer Academic Publishers Press), 321–362. doi: 10.1007/978-1-4020-3218-9_12

Su, M. J., Cai, S. Z., Deng, H. M., Long, C. Y., Ye, C., Song, H. X., et al. (2017). Effects of cadmium and acid rain on cell membrane permeability and osmotic adjustment substance content of *Melia azedarach* L. seedlings. *Acta Sci. Circumstantiae* 37, 4436–4443. doi: 10.13671/j.hjkxxb.2017.0216. (in chinese).

Tang, C. F., Chen, Y. H., Zhang, Q. N., Li, J. B., Zhang, F. Y., and Liu, Z. M. (2019). Effects of peat on plant growth and lead and zinc phytostabilization from lead-zinc mine tailing in southern China: Screening plant species resisting and accumulating metals. *Ecotox. Environ. Safe.* 176, 42–49. doi: 10.1016/j.ecoenv.2019.03.078

Teng, Y., Luo, Y., Ma, W. T., Zhu, L. J., Ren, W. J., Luo, Y. M., et al. (2015). *Trichoderma reesei* FS10-C enhances phytoremediation of Cd-contaminated soil by *Sedum plumbizincicola* and associated soil microbial activities. *Front. Plant Sci.* 6, 438. doi: 10.3389/fpls.2015.00438

Trikshiqi, R., and Rexha, M. (2015). Heavy metal monitoring by Ligustrum lucidum, Fam: Oleaceae vascular plant as bio-indicator in Durres city. *Int. J. Curr. Res.* 7, 14415–14422.

Velikova, V., Tsonev, T., Loreto, F., and Centritto, M. (2011). Changes in photosynthesis, mesophyll conductance to CO_2, and isoprenoid emissions in *Populus nigra* plants exposed to excess nickel. *Environ. Pollut.* 159, 1058–1066. doi: 10.1016/j.envpol.2010.10.032

Wali, M., Gunsè, B., Llugany, M., Corrales, I., Abdelly, C., Poschenrieder, C., et al. (2016). High salinity helps the halophyte Sesuvium portulacastrum in defense against Cd toxicity by maintaining redox balance and photosynthesis. *Planta* 2, 1–14. doi: 10.1007/s00425-016-2515-5

Wang, S. Z., Zhang, D. Y., and Pan, X. L. (2013). Effects of cadmium on the activities of photosystems of Chlorella pyrenoidosa and the protective role of cyclic electron flow. *Chemosphere* 2, 230–237. doi: 10.1016/j.chemosphere.2013.04.070

Yu, P. Y., Sun, Y. P., Huang, Z. L., Zhu, F., Sun, Y. J., and Jiang, L. J. (2019). The effects of ectomycorrhizal fungi on heavy metals' transport in pinus massoniana and bacteria community in rhizosphere soil in mine tailing area. *J. Hazard. Mater* 381, 121203–121215. doi: 10.1016/j.jhazmat.2019.121203

Zhang, H. H., Xu, N., Li, X., Long, J. H., Sui, X., Wu, Y. N., et al. (2018). Arbuscular Mycorrhizal Fungi (*Glomus mosseae*) improves growth, photosynthesis and protects photosystem II in leaves of *Lolium perenne* L. @ in cadmium contaminated soil. *Front. Plant Sci.* 9, 1156. doi: 10.3389/fpls.2018.01156

Zhong, X., Li, Y. T., Che, X. K., Zhang, Z. S., Li, Y. M., Liu, B. B., et al. (2018). Significant inhibition of photosynthesis and respiration in leaves of *Cucumis sativus* L. by oxybenzone, an active ingredient in sunscreen. *Chemosphere* 219, 456–462. doi: 10.1016/j.chemosphere.2018.12.019

Zhou, W. B., Juneau, P., and Qiu, B. S. (2006). Growth and photosynthetic responses of the bloom-forming cyanobacterium Microcystis aeruginosa to elevated levels of cadmium. *Chemosphere* 10, 1738–1746. doi: 10.1016/j.chemosphere.2006.04.078

Zhou, R. H., Kan, X., Chen, J. J., Hua, H. L., Li, Y., Ren, J. J., et al. (2019). Drought-induced changes in photosynthetic electron transport in maize probed by prompt fluorescence, delayed fluorescence, P700 and cyclic electron flow signals. *Environ. Exp. Bot.* 158, 51–62. doi: 10.1016/j.envexpbot.2018.11.005

Zhuang, P., Hu, H. P., Li, Z. A., Zou, B., and McBride, M. B. (2014). Multiple exposure and effects assessment of heavy metals in the population near mining area in south China. *PloS One* 9, 1–11. doi: 10.1371/journal.pone.0094484

Zivcak, M., Brestic, M., Balatova, Z., Drevenakova, P., Olsovska, K., and Kalaji, H. M. (2013). Photosynthetic electron transport and specific photoprotective responses in wheat leaves under drought stress. *Photosynth. Res.* 1–3, 529–546. doi: 10.1007/s11120-013-9885-3

Conflict of Interest: The authors declare that the research was conducted in the absence of any commercial or financial relationships that could be construed as a potential conflict of interest.